

Alma Mater Studiorum Università di Bologna  
Archivio istituzionale della ricerca

Ruthenium(II) Tris-Pyrazolylmethane Complexes in Transfer Hydrogenation Reactions

This is the final peer-reviewed author's accepted manuscript (postprint) of the following publication:

*Published Version:*

Gobbo A., Ma X., Ciancaleoni G., Zacchini S., Biancalana L., Guelfi M., et al. (2023). Ruthenium(II) Tris-Pyrazolylmethane Complexes in Transfer Hydrogenation Reactions. EUROPEAN JOURNAL OF INORGANIC CHEMISTRY, 26(18), 1-13 [10.1002/ejic.202300078].

*Availability:*

This version is available at: <https://hdl.handle.net/11585/938074> since: 2024-02-07

*Published:*

DOI: <http://doi.org/10.1002/ejic.202300078>

*Terms of use:*

Some rights reserved. The terms and conditions for the reuse of this version of the manuscript are specified in the publishing policy. For all terms of use and more information see the publisher's website.

This item was downloaded from IRIS Università di Bologna (<https://cris.unibo.it/>).  
When citing, please refer to the published version.

(Article begins on next page)

This is the final peer-reviewed accepted manuscript of: **A. Gobbo, X. Ma, G. Ciancaleoni, S. Zacchini, L. Biancalana, M. Guelfi, G. Pampaloni, S. P. Nolan, F. Marchetti, "Ruthenium(II) Tris-Pyrazolylmethane Complexes in Transfer Hydrogenation Reactions", Eur. J. Inorg. Chem., 2023, 26, e202300078**

The final published version is available online at:  
<https://doi.org/10.1002/ejic.202300078>

#### Terms of use:

Some rights reserved. The terms and conditions for the reuse of this version of the manuscript are specified in the publishing policy. For all terms of use and more information see the publisher's website.

*This item was downloaded from IRIS Università di Bologna (<https://cris.unibo.it/>)*

***When citing, please refer to the published version.***

# **Ruthenium(II) Tris-Pyrazolylmethane Complexes in Transfer Hydrogenation Reactions**

Dr. Alberto Gobbo,<sup>a,#</sup> Dr. Xinyuan Ma,<sup>b,#</sup> Prof. Gianluca Ciancaleoni,<sup>a,\*</sup> Prof. Stefano Zacchini,<sup>c</sup> Dr.  
Lorenzo Biancalana,<sup>a</sup> Dr. Massimo Guelfi,<sup>a</sup> Prof. Guido Pampaloni,<sup>a</sup> Prof. Steven P. Nolan,<sup>b,\*</sup> and Prof.  
Fabio Marchetti<sup>a,\*</sup>

<sup>a</sup> University of Pisa, Department of Chemistry, and Industrial Chemistry, Via G. Moruzzi 13, I-56124  
Pisa, Italy.

<sup>b</sup> Ghent University, Department of Chemistry and Centre for Sustainable Chemistry, Krijgslaan 281, S-  
3, 9000 Ghent, Belgium.

<sup>c</sup> University of Bologna, Department of Industrial Chemistry “Toso Montanari”, Viale Risorgimento 4,  
I-40136 Bologna, Italy.

<sup>#</sup> A. G. and X. M. contributed equally to this work.

## **Corresponding Authors**

\*E-mail addresses: [gianluca.ciancaleoni@unipi.it](mailto:gianluca.ciancaleoni@unipi.it); [steven.nolan@ugent.be](mailto:steven.nolan@ugent.be); [fabio.marchetti@unipi.it](mailto:fabio.marchetti@unipi.it)

Web: [https://people.unipi.it/fabio\\_marchetti/](https://people.unipi.it/fabio_marchetti/)

## Abstract

While ruthenium(II) arene complexes have been widely investigated for their potential in catalytic transfer hydrogenation, studies on homologous compounds replacing the arene ligand with the six-electron donor tris(1-pyrazolyl)methane (tpm) are almost absent in the literature. The reactions of  $[\text{RuCl}(\kappa^3\text{-tpm})(\text{PPh}_3)_2]\text{Cl}$ , **1**, with a series of nitrogen ligands (L) proceeded with selective  $\text{PPh}_3$  mono-substitution, affording the novel complexes  $[\text{RuCl}(\kappa^3\text{-tpm})(\text{PPh}_3)(\text{L})]\text{Cl}$  (L = NCMe, **2**; NPh, **3**; imidazole, **4**) in almost quantitative yields. Products **2-4** were fully characterized by IR and multinuclear NMR spectroscopy, moreover the molecular structure of **4** was ascertained by single crystal X-ray diffraction. Compounds **2-4** were evaluated as catalytic precursors in the transfer hydrogenation of a series of ketones with isopropanol as the hydrogen source, and **2** exhibited the highest activity. Extensive NMR experiments and DFT calculations allowed to elucidate the mechanism of the transfer hydrogenation process, suggesting the crucial role played by the tpm ligand, reversibly switching from tri- to bidentate coordination during the catalytic cycle.

## 1. Introduction

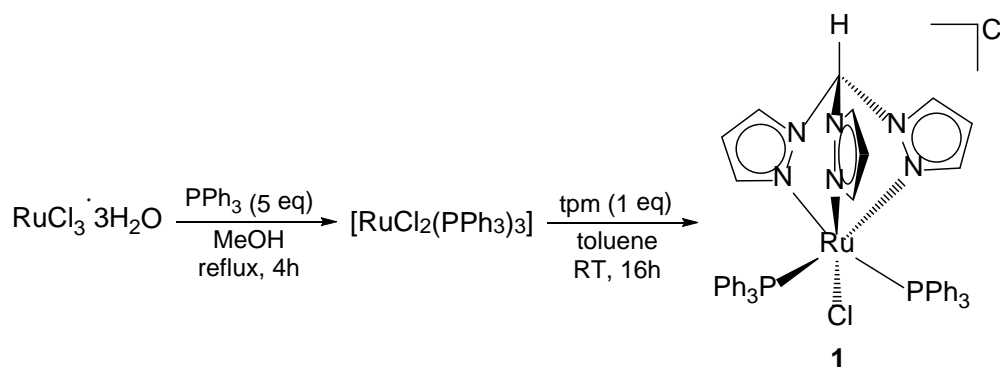
The reduction of carbonyl functions to alcohols via transfer hydrogenation (TH) provides the access to high-value compounds with important applications as natural products, pharmaceuticals, agrochemicals and other fine chemicals.<sup>1,2,3,4,5,6</sup> Isopropanol is easily available and relatively nontoxic, and its use as a solvent for organic transformations has spread out in accordance with the principles of green chemistry and sustainability;<sup>7,8</sup> using isopropanol as solvent for TH is particularly convenient, since it behaves as the hydrogen-donor favouring the conversion of the starting ketone into the targeted alcohol product. There has been an impressive growth in the various transition metal complexes (e.g. rhodium, iridium and rhenium) employed as catalytic precursors for the TH of ketones from isopropanol.<sup>9,10,11,12,13</sup> Among them, ruthenium compounds have played a leading role,<sup>15,16,17,18</sup> and

related work in this area by Noyori was awarded with the Nobel Prize in 2001.<sup>19</sup> A considerable number of ruthenium(II) arene complexes, bearing a wide diversity of co-ligands, has been intensively investigated, showing a variable catalytic activity.<sup>20,21,22,23,24,25,26,27,28</sup> The Tóuge group developed bifunctional Ru complexes, bearing an ether linkage between 1,2-diphenylethylenediamine (DPEN) and the  $\eta^6$ -arene ligand, that catalyse TH with excellent enantioselectivity under mild reaction conditions.<sup>29</sup> In 2020, the reduction of ketones mediated by ruthenium(II) *p*-cymene complexes, containing quinoxalin-11-one derivatives or tryptanthrin-6-oxime, was reported by Potapov and Benassi, resulting in a good catalytic activity with 2-propanol as the hydrogen donor.<sup>30</sup> Subsequently, the same group successfully synthesized a series of mono- and dinuclear arene-ruthenium (II) complexes with imidazole-containing ligands and applied them as efficient catalysts in the TH reaction.<sup>31</sup> In spite of these relatively recent developments, the exploration of novel catalysts and mechanistic features remains of high interest.

Tris(pyrazolyl)methane (tpm) and related substituted molecules may be considered as arene surrogates, in that both types of compounds are neutral and can behave as six-electron donor ligands towards transition metal centres.<sup>32,33</sup> Indeed, tripodal coordination involving three nitrogen atoms ( $\kappa^3$ ) is common for the tpm ligand, usually providing a substantial robustness to the resulting complexes, although alternative coordination fashions are also feasible.<sup>34,35,36</sup> Several complexes with tpm or substituted analogues, based on different transition metals, have been investigated as catalytic precursors in a variety of organic transformations.<sup>37,38,39,40</sup> The interchange between tri- and bidentate coordination is generally assumed to play an important role in the catalytic activity,<sup>40</sup> nevertheless this feature has been rarely ascertained in the literature. Jagirdar and co-workers showed that an iridium-tpms complex (tpms = tris(pyrazolyl)methanesulfonate) catalysed the hydrogenation of 3,3-dimethyl-1-butene, and hypothesized that the reaction proceeded through a  $\kappa^2$ -tpms intermediate based on DFT calculations.<sup>41</sup>

There are several examples of ruthenium-tpm complexes investigated in catalysis;<sup>42,43,44,45,46,47</sup> however, in sharp contrast with the related arene systems, ruthenium-tpm compounds have been almost unexplored for their potential in hydrogenation reactions. Studies concerning TH activity of ruthenium-tpm species have been limited to the hydrogenation of acetophenone by the nitrosyl complex  $[\text{RuCl}_2(\text{NO})(\kappa^3\text{-tpm})]\text{PF}_6$  and its tris(3,5-dimethyl-1-pyrazolyl)analogue,<sup>48</sup> both obtained from  $[\text{RuCl}_3(\text{NO})]$ ;<sup>49</sup> nevertheless, the activity was poor and the catalytic pathway was not elucidated.

In the present work, we selected  $[\text{RuCl}(\kappa^3\text{-tpm})(\text{PPh}_3)_2]\text{Cl}$ , **1**, as a convenient entry to access three novel  $\text{Ru}^{\text{II}}$ -tpm compounds by means of triphenylphosphine substitution with nitrogen ligands. Complex **1** is easily prepared from commercial ruthenium trichloride via an optimized two-step route recently reported by some of us (Scheme 1).<sup>50,51</sup> Subsequently, **1** and derivatives were investigated as catalysts for the transfer hydrogenation of a range of ketones from isopropanol, disclosing the important role of the tpm ligand.



**Scheme 1.** Two-step synthesis of ruthenium(II) tris(pyrazolyl)methane complex used as starting material for the synthesis of catalysts investigated in this work.

## 2. Results and discussion

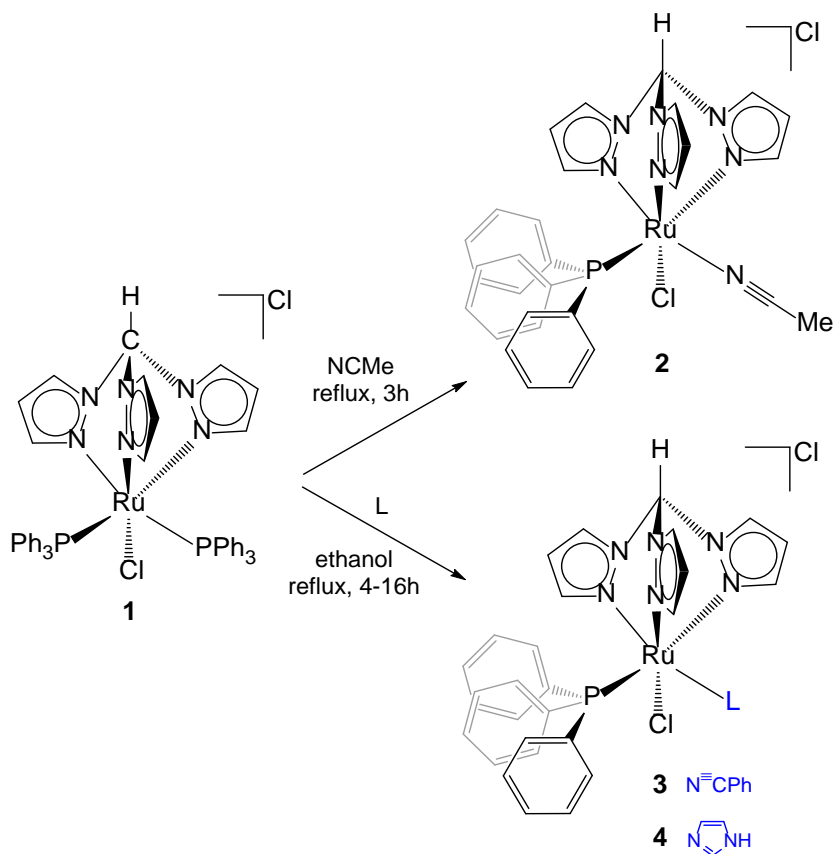
### 2.1. Synthesis and structural characterization of complexes

When the bis-triphenylphosphine complex **1** was heated at reflux temperature in acetonitrile, quantitative  $\text{PPh}_3/\text{NCMe}$  replacement occurred in 3 hours, and the acetonitrile adduct **2** was isolated in 95% yield after work-up (Scheme 2). This result is not common, in that nitrile ligands are easily

replaced by phosphines in group 8<sup>52,53,54</sup> and other transition metal complexes.<sup>55,56</sup> It is envisaged that the clean PPh<sub>3</sub>/NCMe substitution is driven by the large excess of nitrile and the steric demand exerted by two bulky triphenylphosphine ligands occupying adjacent coordination sites in **1**, that was previously inferred to explain the restricted rotation around the Ru-P bonds.<sup>50</sup>

When **2** was heated in ethanol solution in the presence of one equivalent of triphenylphosphine, 50% conversion of **2** into **1** was recognized by <sup>31</sup>P{<sup>1</sup>H}NMR after 3 hours, evidencing some labile character of the NCMe ligand.

On the other hand, the reactions of **1**, in refluxing ethanol, with equimolar amounts of benzonitrile and imidazole afforded complexes **3-4** in 90-94% yields (Scheme 2).



**Scheme 2.** Synthesis of ruthenium(II) tris(pyrazolyl)methane complexes obtained via PPh<sub>3</sub> substitution with N-donors.

The novel complexes **2-4** are air-stable yellow solids, which are soluble in methanol, dichloromethane and chloroform, and insoluble in diethyl ether, pentane and toluene. They were fully characterized in

the solid state by elemental analysis and IR spectroscopy (Figures S1-S4 in the Supporting Information), and in CDCl<sub>3</sub> solution by multinuclear NMR spectroscopy (Figures S6-S16). The IR spectra of **2** and **3** display the diagnostic absorption related to the nitrile function at 2278 and 2247 cm<sup>-1</sup>, respectively.

The NMR spectra of **2-4** display a single set of resonances, and signals related to the tpm ligand do not significantly differ in **2-4**. Specifically, the ring carbons resonate in the intervals 144.2-148.6 ppm, 132.8-135.7 ppm and 108.1-108.6 ppm, while the signal of the methylidyne carbon occurs at ca. 74 ppm. The <sup>31</sup>P{<sup>1</sup>H} resonance for the phosphorus nucleus undergoes a notable shift on going from **1** (39.5 ppm) to the products **2-4** (46.5-51.7 ppm).

Crystals of **4** suitable for X-ray analysis were collected by slow diffusion technique (Figure 1). Complex **4** displays a distorted octahedral geometry, as found in the precursor **1** and related complexes.<sup>50,57,58,59</sup> The Ru(1)-Cl(1) distance [2.389(5) Å] is comparable to that found in **1** [2.402(2) Å], whereas the Ru(1)-P(1) distance [2.289(5) Å] is slightly shorter [2.651(2) and 2.374(2) Å in **1**]. The replacement of a bulky PPh<sub>3</sub> ligand in **1** with the less sterically demanding imidazole ligand causes the P(1)-Ru(1)-X angle [X = P, 103.9(1)° for **1**; N, 93.7(4)° for **4**] to approach 90° in **4** compared to **1**. The N-Ru-N angles involving the tridentate trispyrazolylmethane ligand are all smaller than the ideal value of 90° expected for an octahedral complex.<sup>50</sup> The imidazole N(8)-H(8) group of **4** is involved in a hydrogen bond with the chloride counter-ion [N(8)-H(8) 0.88 Å, H(8)⋯Cl(2) 2.30 Å, N(8)⋯Cl(2) 3.107(16) Å, N(8)-H(8)-Cl(2) 153.1°].



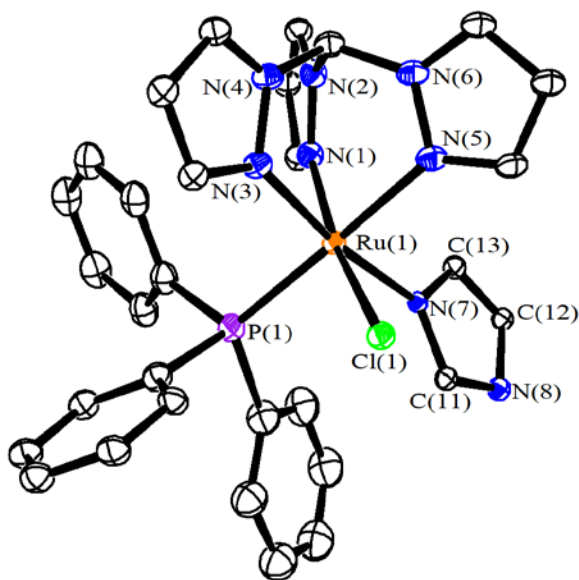


**Figure 1.** View of the molecular structure of the cation of **4**. Displacement ellipsoids are at the 50% probability level. Selected bond lengths (Å) and angles (°): Ru(1)-N(1) 2.099(17), Ru(1)-N(3) 2.093(15), Ru(1)-N(5) 2.123(16), Ru(1)-N(7) 2.090(14), Ru(1)-Cl(1) 2.389(5), Ru(1)-P(1) 2.289(5), N(7)-C(11) 1.33(2), C(11)-N(8) 1.34(2), N(8)-C(12) 1.36(2), C(12)-C(13) 1.34(2), C(13)-N(7) 1.36(3), N(1)-Ru(1)-N(3) 85.1(6), N(1)-Ru(1)-N(5) 85.2(6), N(3)-Ru(1)-N(5) 85.4(6), P(1)-Ru(1)-Cl(1) 95.41(18), P(1)-Ru(1)-N(7) 93.7(4), Cl(1)-Ru(1)-N(7) 87.4(4). CCDC: 2168078.

Further, the behaviour of **1-4** in deuterated water was assessed by NMR spectroscopy (see Section 4 in the Experimental for details). Thus, **2** and **4** are slightly soluble in D<sub>2</sub>O (ca. 4·10<sup>-3</sup> M), while **1** and **3** are insoluble. Compounds **2** and **4** exist in aqueous solution in equilibrium with the respective chloride/water exchange adducts (see Figures S17-S18 in the Supporting Information), in accordance with previous results on related complexes.<sup>50</sup> The relative amount of aquo-complex, after 2 hours from the dissolution in D<sub>2</sub>O, is 80% and 46% for **2** and **4** respectively. This outcome highlights the influence of electronic factors arising from the nitrogen ligand in **2-4** on the kinetics of chloride dissociation reactions, that might be relevant to the catalytic activity (*vide infra*).

## 2.2. Catalytic activity in transfer hydrogenation

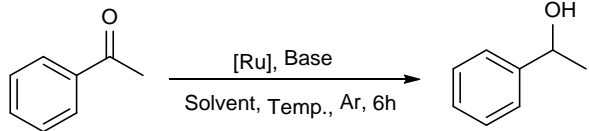
With complexes **1-4** in hand, their catalytic activity in the transfer hydrogenation (TH) of ketones was explored. Initially, the TH reaction was tested using the model substrate acetophenone, 10 mol% of

KOH as the base, and 1 mol% loading of ruthenium(II) arene complex **2** in *i*PrOH at 80 °C under Ar, leading to moderate yield of 1-phenylethan-1-ol after 6h (Table 1, entry 1). Then, when the amount of base was increased to 50 mol%, the conversion of the reaction was not greatly improved (Table 1, entry 2). Based on these early results, we explored the effect of different bases (Table 1, entries 3-6). Monitoring the reaction by <sup>1</sup>H NMR spectroscopy allowed us to observe complete conversion in the presence of NaOH as the base after 6 h. On the other hand, traces or no hydrogenation products were detected when weak bases were used. The reaction still yielded 99% NMR yield when reducing the amount of NaOH to 10 mol% (Table 1, entries 7-9). Decreasing the catalyst loading by half resulted in a dramatic drop in productivity (Table 1, entry 10). However, a similar result was obtained by increasing the catalyst loading from 1 mol% to 1.5 mol% (Table 1, entry 11). Low reaction yields were obtained when we performed the reaction with other protic solvents instead of isopropanol (Table 1, entries 12-14).

Subsequently, we investigated the effect of different ruthenium-tpm catalysts on the model TH reaction (Table 1, entries 15-17). Among the catalysts examined, **1** and **4** exhibited lower catalytic performances than **2** and **3**, which is probably due to a different mechanism of reaction (*vide infra*).<sup>60</sup> The performance of the benzonitrile catalyst **3** is slightly worse compared to the acetonitrile catalyst **2** (compare entries 8 and 16 in Table 1). Conducting the reaction in air hindered the progress of the reaction (possibly due to NaOH carbonation and/or air sensitivity of intermediate ruthenium species), and only a 28% yield was obtained after a reaction conducted overnight (Table 1, entry 18). In addition, product formation was reduced with decreasing reaction temperature or reaction time, resulting in moderate yields (Table 1, entries 19-20).

By comparing analogous experimental conditions, the activity provided by complex **2** in the TH of acetophenone, under optimized conditions, is exceedingly higher than that previously reported for the only other ruthenium-tpm compound previously assessed for the same reaction, i.e. [RuCl<sub>2</sub>(NO)(κ<sup>3</sup>-tpm)]PF<sub>6</sub>,<sup>48</sup> and promising when compared to recently reported ruthenium(II) arene systems.<sup>61,62</sup>

**Table 1.** Optimization of the reaction conditions for the conversion of acetophenone into 1-phenylethan-1-ol.<sup>a</sup> Optimal reaction conditions are reported as entry 8 (see also Table S1).

					
Entry	Ru cat. (mol%)	Base (mol%)	Solvent	Temp. (°C)	Yield (%) <sup>b</sup>
1	<b>2</b> (1 mol%)	KOH (10 mol%)	<i>i</i> PrOH	80	55
2	<b>2</b> (1 mol%)	KOH (50 mol%)	<i>i</i> PrOH	80	74
3	<b>2</b> (1 mol%)	K <sub>2</sub> CO <sub>3</sub> (50 mol%)	<i>i</i> PrOH	80	<10
4	<b>2</b> (1 mol%)	NaOAc (50 mol%)	<i>i</i> PrOH	80	-
5	<b>2</b> (1 mol%)	NaOH (50 mol%)	<i>i</i> PrOH	80	99
6	<b>2</b> (1 mol%)	<i>t</i> BuOK (50 mol%)	<i>i</i> PrOH	80	83
7	<b>2</b> (1 mol%)	NaOH (20 mol%)	<i>i</i> PrOH	80	98
<b>8</b>	<b>2</b> (1 mol%)	<b>NaOH (10 mol%)</b>	<b><i>i</i>PrOH</b>	<b>80</b>	<b>99</b>
9	<b>2</b> (1 mol%)	NaOH (5 mol%)	<i>i</i> PrOH	80	57
10	<b>2</b> (0.5 mol%)	NaOH (10 mol%)	<i>i</i> PrOH	80	18
11	<b>2</b> (1.5 mol%)	NaOH (10 mol%)	<i>i</i> PrOH	80	>99
12	<b>2</b> (1 mol%)	NaOH (10 mol%)	EtOH	80	trace
13	<b>2</b> (1 mol%)	NaOH (10 mol%)	MeOH	65	15
14	<b>2</b> (1 mol%)	NaOH (10 mol%)	H <sub>2</sub> O	100	-
15	<b>1</b> (1 mol%)	NaOH (10 mol%)	<i>i</i> PrOH	80	62
16	<b>3</b> (1 mol%)	NaOH (10 mol%)	<i>i</i> PrOH	80	80
17	<b>4</b> (1 mol%)	NaOH (10 mol%)	<i>i</i> PrOH	80	26
18 <sup>c</sup>	<b>2</b> (1 mol%)	NaOH (10 mol%)	<i>i</i> PrOH	80	28
19	<b>2</b> (1 mol%)	NaOH (10 mol%)	<i>i</i> PrOH	60	56
20 <sup>d</sup>	<b>2</b> (1 mol%)	NaOH (10 mol%)	<i>i</i> PrOH	80	60

<sup>a</sup> Reaction conditions: acetophenone (0.3 mmol, 1 eq.), base, Ru catalyst, *i*PrOH (1.5 mL), 6 h, under Ar. <sup>b</sup> NMR yields (1,3,5-trimethoxybenzene as internal standard). <sup>c</sup> Under air, overnight. <sup>d</sup> Reaction time is 4 h.

Several ketones were employed to explore the range of catalyst application for transfer hydrogenation. The results are shown in Table 2. The ruthenium(II) arene complex **2** showed high catalytic activity and conversion to aryl ketones. In fact, almost all substrates bearing various substituents can be

converted to the corresponding alcohols in good to excellent yields. By comparison, the reaction efficiency with halide-functionalized acetophenone was slightly lower. In contrast, the use of bis(4-fluorophenyl)methanone as a substrate facilitated the conversion of ketone to alcohol and led to a 91% isolated yield. Electron-donating groups (-OMe) provide limited reaction efficiency and a longer time is required to reach good conversion.

Unfortunately, aliphatic ketones, such as cyclohexanone and pentanone, do not produce the corresponding alcohols under optimal conditions, which may be associated with the very different electronic effects of the ketone structure.<sup>63,64</sup>

**Table 2.** Transfer hydrogenation of ketones catalysed by complex **2** under optimized reaction conditions.<sup>a</sup>

$  \text{R}'\text{-C}_6\text{H}_4\text{-C(=O)R} \xrightarrow[\text{iPrOH (2 ml), 80}^\circ\text{C, 6h}]{\text{2 (1 mol\%), NaOH (10 mol\%)}} \text{R}'\text{-C}_6\text{H}_4\text{-CH(OH)R}  $			
Entry	Substrate	Product	Yield <sup>b</sup>
1			91
2			88
3			79
4			87
5			76 <sup>c</sup>
6			91



<sup>a</sup> Reaction conditions: ketone (0.5 mmol, 1 eq.), NaOH (10 mol%), catalyst **2** (1 mol%), <sup>i</sup>PrOH (2.0 mL), 80 °C, 6 h, under Ar. <sup>b</sup> Isolated yields. <sup>c</sup> 12 h.

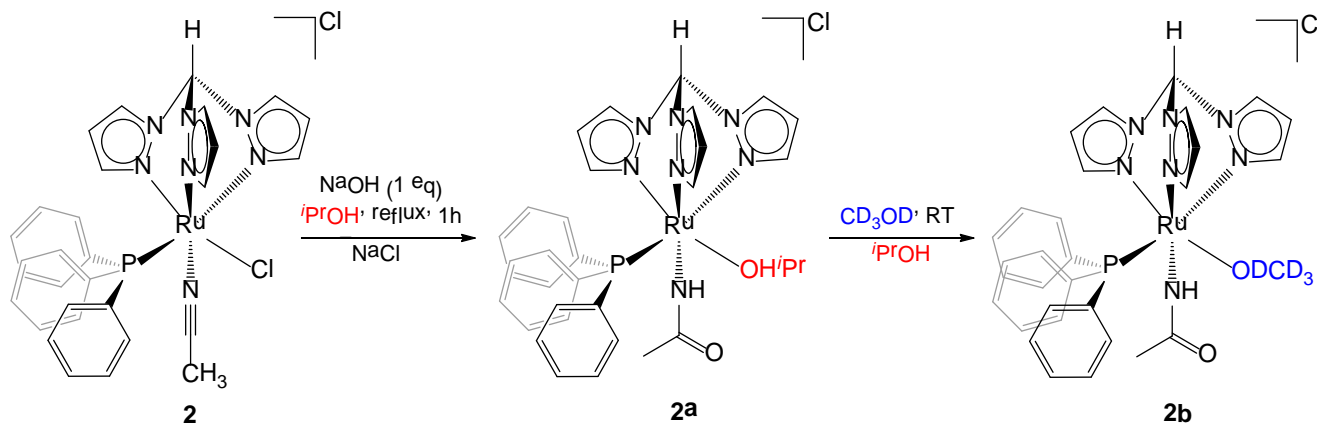
### 2.3. NMR studies

The mechanism of the transfer hydrogenation reaction promoted by the most active catalyst, **2**, was investigated by NMR spectroscopy and DFT calculations. First, an isopropanol solution of **2** was heated at reflux in the presence of one equivalent of sodium hydroxide, thus reproducing the conditions of the catalytic reactions but in the absence of the organic substrate. After thorough removal of the volatiles under vacuum, the residue was redissolved in CD<sub>3</sub>OD. Subsequent NMR experiments (Figures S31-S33) showed the prevalent formation of a new ruthenium derivative, lacking acetonitrile, and the presence in solution of one equivalent of isopropanol. This experiment was repeated multiple times, revealing a substantial reproducibility. Experimental facts suggest the conversion of **2** into the acetamido complex [Ru{κ*N*-NHC(=O)CH<sub>3</sub>}(κ<sup>3</sup>-tpm)(PPh<sub>3</sub>)(<sup>i</sup>PrOH)]Cl, **2a**, via nitrile hydroxylation and chloride/isopropanol substitution (Scheme 3). The dissociation of the phosphine ligand was ruled out based on <sup>31</sup>P NMR spectroscopy. By dissolving **2a** into deuterated methanol required for NMR analysis, the isopropanol ligand is expected to be released into the solution and replaced by one solvent molecule (formation of **2b**, Scheme 3).

Note that a variety of ruthenium compounds are able to promote the hydration of nitriles,<sup>65,66,67,68,69</sup> and thus several ruthenium-acetamido complexes have been reported.<sup>70,71,72,73</sup> In particular and analogously to the present case, the acetamido complex [RuH(κ*N*-NHCOMe)(PCy<sub>3</sub>)<sub>2</sub>(<sup>i</sup>PrOH)(CO)], containing an isopropanol co-ligand, was obtained from the acetonitrile precursor [RuH(NCCH<sub>3</sub>)<sub>2</sub>(PCy<sub>3</sub>)<sub>2</sub>(CO)]BF<sub>4</sub>

by reaction with KOH in isopropanol.<sup>70</sup> Interestingly,  $[\text{RuH}(\text{NHCOMe})(\text{PCy}_3)_2(^i\text{PrOH})(\text{CO})]$  works as an efficient catalyst in the TH of aromatic ketones from isopropanol.

The IR spectrum of solid **2a** displays multiple bands between 1665 and 1545  $\text{cm}^{-1}$ , ascribable to the amide carbonyl stretching, and a broad absorption centred at 3317  $\text{cm}^{-1}$  which accounts for the isopropanol ligand (Figure S5). In the  $^1\text{H}$  and  $^{13}\text{C}$  NMR spectra (**2b**), diagnostic signals assigned to the coordinated acetamide occur at 5.68 ppm (NH) and 184.4-184.3 ppm (C=O); moreover, a HMBC correlation has been found between the  $^{13}\text{C}$  signal due to the carbonyl and the  $^1\text{H}$  signal due to the methyl (1.94-1.93 ppm). The NH resonance has lower intensity than expected, suggesting the occurrence of H-D exchange in  $\text{CD}_3\text{OD}$ .<sup>70</sup> This phenomenon might also explain the splitting of the resonances due to the methyl and carbonyl groups. Compound **2a** is poorly soluble and unstable in chlorinated solvents, as the initial pale yellow-green solution turned dark-green within a few minutes. Nevertheless,  $^1\text{H}$  NMR spectrum registered in  $\text{CD}_2\text{Cl}_2$  soon after the preparation of the sample showed the NH resonance at ca. 4.4 ppm, in agreement with literature data (see Experimental).<sup>70,71</sup>



**Scheme 3.** Formation of the acetamido complex **2a** via nitrile ligand transformation, and subsequent exchange of solvent ligand. **2a** analysed by solid state IR spectroscopy, **2b** by multinuclear NMR spectroscopy.

When the reaction of **2** with NaOH/*i*-PrOH (Scheme 3) was performed in the presence of 2 eq. of acetophenone, partial conversion of acetophenone to 1-phenylethanol was recognized (approximately 64%), while **2a** remained the predominant ruthenium species in solution ( $^1\text{H}$ ,  $^{13}\text{C}$  and  $^{31}\text{P}$  NMR spectra recorded in  $\text{CD}_3\text{OD}$ ). Moreover,  $^1\text{H}$  NMR spectroscopy revealed the minor formation (approximately

14% with respect to **2a**) of a ruthenium-hydride species, manifested by a doublet at -13.87 ppm in CD<sub>3</sub>OD. The value of the coupling constant ( $^2J_{\text{HP}} = 28.8$  Hz) resembles that previously reported for a similar {H-Ru-PPh<sub>3</sub>} system ( $^2J_{\text{HP}} = 27.8$  Hz in acetone-d<sub>6</sub>).<sup>74</sup>

Combined, NMR experiments on the nitrile complex **2** and literature facts suggest that the active species involved in the catalytic cycle is an acetamido complex, thus the higher reactivity of **2** should not be ascribed to some labile character of the acetonitrile ligand, otherwise observed in coordination chemistry.<sup>52,53,54</sup>

## 2.4. DFT calculations

Based on the results of the NMR study, DFT calculations were performed replacing the bulky PPh<sub>3</sub> ligand with PH<sub>3</sub>, to optimize the computational resources. Thus, starting from the model complex [RuCl( $\kappa^3$ -tpm)(PH<sub>3</sub>)(NCMe)]<sup>+</sup> (**2<sub>PH3</sub>**<sup>+</sup>), the hydroxide can displace the chloride ligand giving [Ru(OH)( $\kappa^3$ -tpm)(PH<sub>3</sub>)(NCMe)]<sup>+</sup> (**Int1**, Figure 2), which is 20.4 kcal/mol more stable than **2<sub>PH3</sub>**<sup>+</sup> in terms of free Gibbs energy. Intramolecular attack of the hydroxide ligand in **Int1** to the nitrile function proceeds with an activation barrier of 20.3 kcal/mol (**TS1**). The same step has been invoked also for the nitrile hydration of other ruthenium(II) complexes.<sup>70,71</sup> The kinetic product is [Ru( $\kappa^3$ -tpm)(PH<sub>3</sub>)( $\kappa^2$ -NC(OH)Me)]<sup>+</sup> (**Int2**,  $\Delta G = -0.5$  kcal/mol) containing a bidentate N,O-ligand,<sup>75</sup> but the enol-to-keto tautomerization leads to the more stable [Ru( $\kappa^3$ -tpm)(PH<sub>3</sub>)( $\kappa^2$ -NHC(=O)Me)]<sup>+</sup> (**Int2a**,  $\Delta G = -28.3$  kcal/mol). Such tautomerism was previously observed in other Ru-tpm systems,<sup>76</sup> and is consistent with the NMR detection of **2a** (see NMR studies).

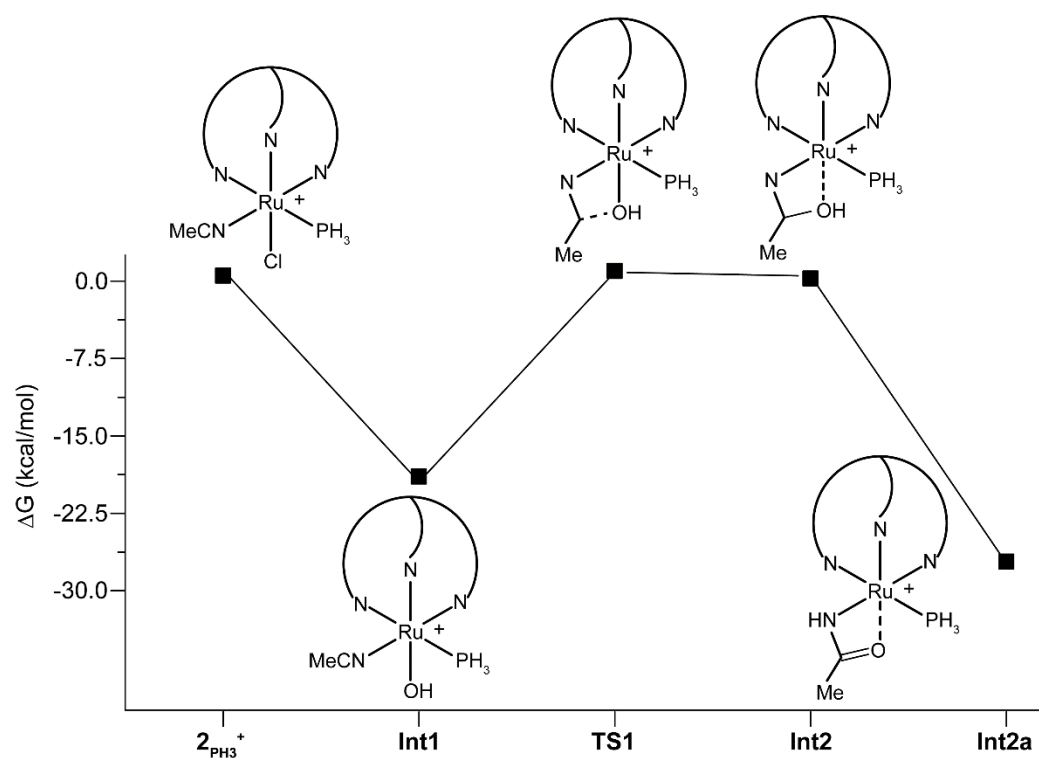


**Figure 2.** Energy profile for the activation of the model pre-catalyst  $2_{\text{PH}_3}^+$  under basic conditions.

Once **Int2a** is formed, isopropanol can coordinate the metal centre through the alcoholic group (**Int3**, Figure 3). Possible adducts alternative to **Int3** were considered and resulted less favourable (see Figure S34 in the Supporting Information). Under the basic conditions experimentally used in catalysis, the isopropanol ligand in **Int3** is deprotonated with a free energy gain of 30.7 kcal/mol (**Int4**).<sup>77</sup> Then, the vacancy required to carry on the reaction may be generated by the tpm ligand, switching from  $\kappa^3$  to  $\kappa^2$  coordination mode.<sup>78</sup> Indeed, an interaction between the isopropanol CH hydrogen and the metal can be established (**TS2**,  $\Delta G^\ddagger = 19.0$  kcal/mol with respect to **Int4**, -11.7 kcal/mol with respect to **Int3**), leading to the acetone derivative  $[\text{RuH}(\kappa^2\text{-tpm})(\text{NHCOMe})(\text{O}=\text{CMe}_2)(\text{PH}_3)]$  (**Int5**) via  $\beta$ -elimination. At this point, acetophenone may displace the acetone ligand (**Int6**) and subsequently add the ruthenium-bound hydride through **TS3** ( $\Delta G^\ddagger = 4.6$  kcal/mol). The resulting intermediate (**Int7**) contains a 1-phenyl-ethoxideligand and the tpm ligand still in a  $\kappa^2$  coordination mode. Finally, the tpm restores



the  $\eta^3$  coordination mode, and **Int8** is more stable than **Int4** by 4.4 kcal/mol, providing the thermodynamic driving force to the overall process. The visual inspection of optimized geometries does not reveal importance of the steric hindrance of the phosphine, therefore  $\text{PH}_3$  can be considered a satisfying model for the bulkier  $\text{PPh}_3$ . Note that, starting from **Int3**, the coordination vacancy for hydride abstraction might be in principle generated by intramolecular proton transfer from isopropanol to amide, giving an isopropoxide ligand and releasing acetamide from coordination. However, this process resulted much less favoured than **TS2**, with  $\Delta G^\ddagger = +7.1$  kcal/mol with respect to **Int3**.

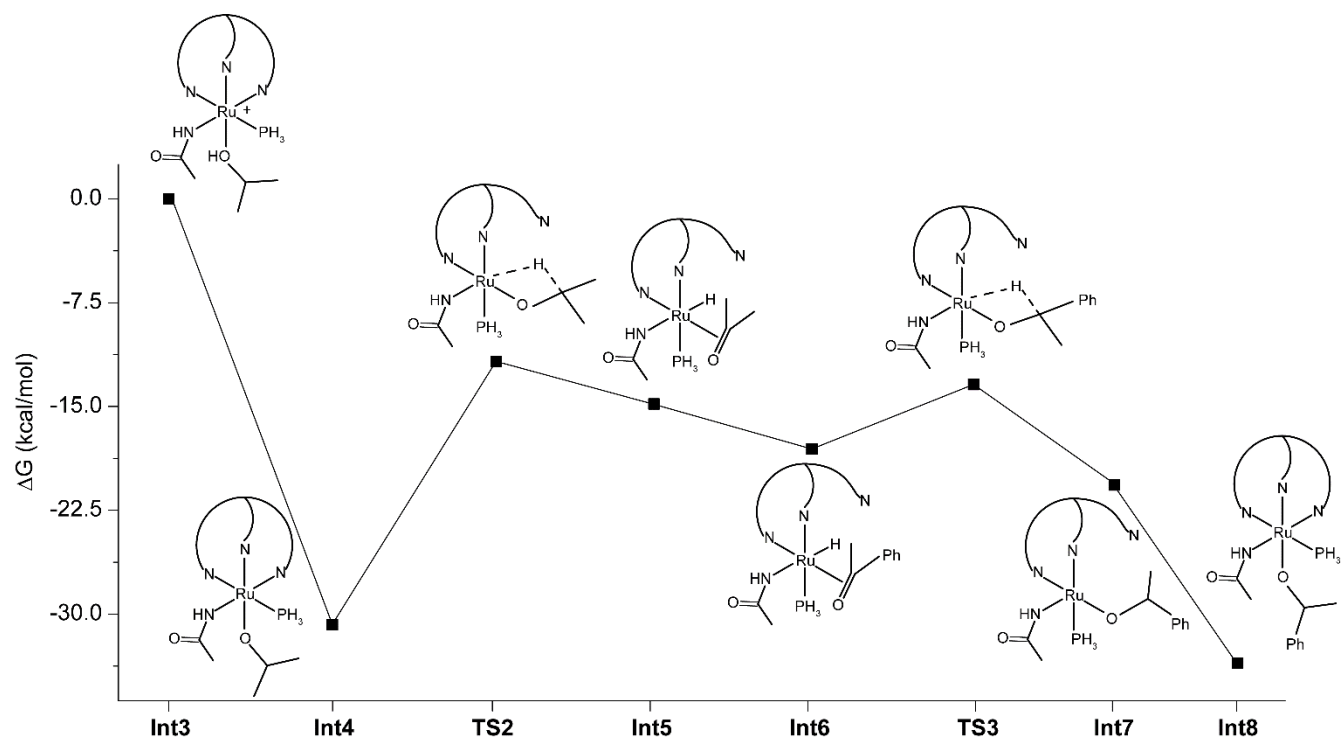


**Figure 3.** Energy profile for the transfer hydrogenation of acetophenone mediated by a model ruthenium-tpm system.

In summary, based on the experimental (NMR) and theoretical (DFT) results, a catalytic cycle for the transfer hydrogenation of ketones from isopropanol, promoted by the best catalyst **2** in the presence of  $\text{NaOH}$ , is proposed (Figure 4). The resting species corresponds to deprotonated **2a** (see Scheme 3) and is formed via hydroxide addition to the acetonitrile and chloride-isopropoxide substitution, assisted by the

basic environment. The subsequent  $\beta$ -elimination step from isopropoxide is allowed by the switch of the tpm ligand from  $\kappa^3$  to  $\kappa^2$  coordination, to give a ruthenium-hydride. The reacting ketone (e.g., acetophenone) replaces the newly generated acetone ligand, and carbonyl hydrogenation by the hydride takes place.

Remarkably, the tris-pyrazolylborate complex  $[\text{RuH}(\text{Tp})(\text{PPh}_3)(\text{NCMe})]$  was previously reported to promote the hydrogenation of carbon dioxide to formic acid, and the proposed mechanism involves acetonitrile displacement and no switch of the tridentate Tp ligand.<sup>59</sup>

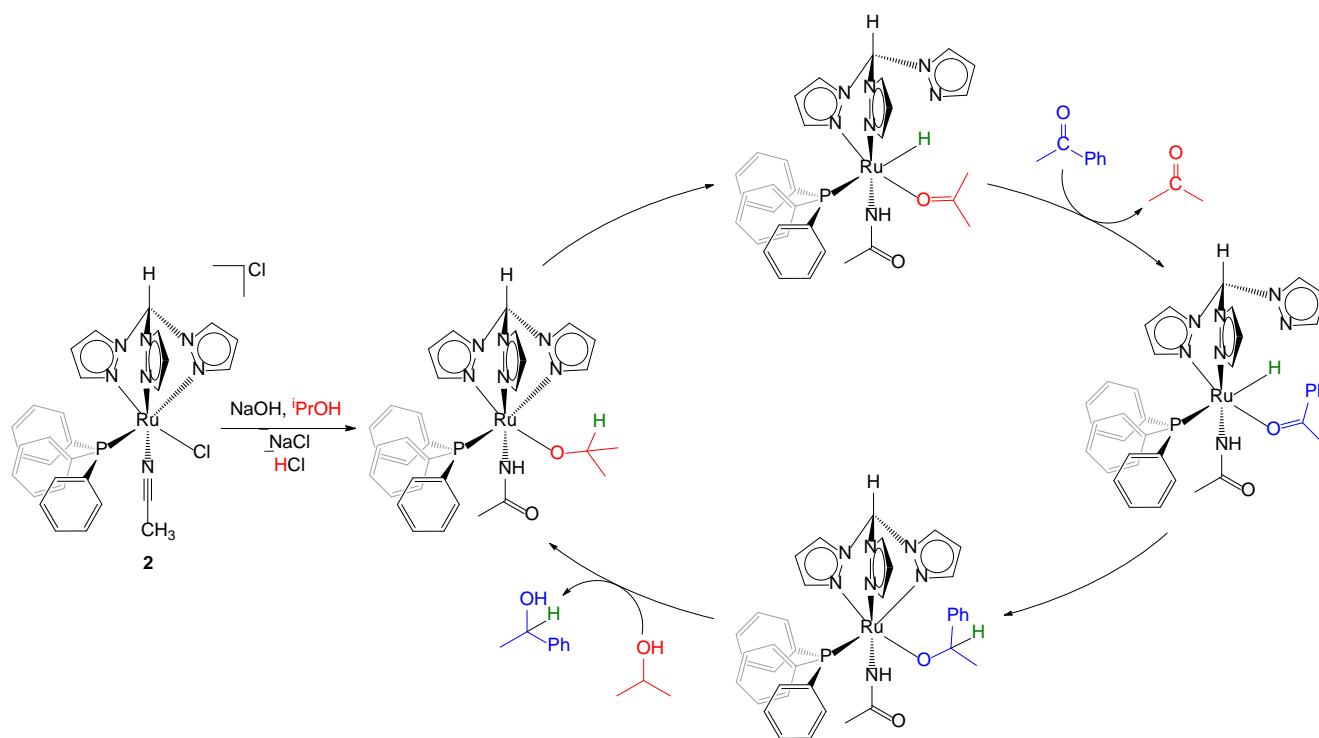


**Figure 4.** Proposed mechanism for the transfer hydrogenation of acetophenone by complex **2**.

Benzonitrile may undergo facile metal-mediated hydroxylation likewise acetonitrile.<sup>79</sup> Indeed, when a 2-propanol solution of **3** was heated at reflux in the presence of one equivalent of sodium hydroxide, 70% conversion to the corresponding benzamido complex was recognized by NMR. However, catalyst **3** is slightly less efficient than **2** (Table 1), possibly due to electronic factors related to the benzamido ligand compared to the acetamido, slowing down ligand dissociation steps.

The lower activity exhibited by  $[\text{RuCl}(\kappa^3\text{-tpm})(\text{PPh}_3)(\text{L})]\text{Cl}$  ( $\text{L} = \text{PPh}_3$ , **1**; imidazole, **4**) seems ascribable to a different mechanism, consisting in the dissociation of  $\text{L}$  and preserving the  $\kappa^3$ -coordination of  $\text{tpm}$  during the catalytic cycle. As a matter of fact, a  $^{31}\text{P}$  NMR experiment conducted on a solution of **1** in  $i\text{PrOH}/\text{NaOH}$  clearly pointed out the release of  $\text{PPh}_3$  (ca. 62%) and the likely formation of  $[\text{RuCl}(\text{O}^i\text{Pr})(\kappa^3\text{-tpm})(\text{PPh}_3)]$ ; under analogous conditions, **4** afforded a mixture of compounds arising from imidazole elimination (see Experimental). DFT calculations confirmed that **1** and **4** undergo substitution of  $\text{L}$  by isopropoxide from the solution. Considering the steric hindrance around the metal, the mechanism of this substitution must be dissociative. The  $\Delta G$  is +24.6 kcal/mol for  $\text{PH}_3$  dissociation from the model compound  $[\text{RuCl}(\kappa^3\text{-tpm})(\text{PH}_3)_2]^+$ , and this is the rate determining step of the whole process. Successively, isopropoxide coordinates to the metal, giving  $[\text{RuCl}(\text{O}^i\text{Pr})(\kappa^3\text{-tpm})(\text{PH}_3)]$  ( $\Delta G = -13$  kcal/mol). Then, to generate the coordination vacancy enabling hydride elimination from the isopropoxide, the chloride ligand moves to the second coordination sphere ( $\Delta G^\ddagger = 14.3$  kcal/mol). Otherwise,  $\text{tpm}$  switching to  $\kappa^2$ -coordination mode would involve a more prohibitive barrier (19.5 kcal/mol).

### 3. Conclusions

Transfer hydrogenation of ketones from isopropanol is a reaction of tremendous impact for which the exploration of new metal catalysts and mechanistic features is of currently great interest. In contrast with the related Ru-arene compounds, ruthenium(II) tris(pyrazolyl)methane compounds have been substantially under explored for their catalytic potential. Herein, we describe a straightforward method to access new complexes of such type with different nitrogen ligands, and a study of their activity in the transfer hydrogenation of a range of ketones. All investigated compounds showed activity under basic conditions, and the acetonitrile adduct emerged as the most performant catalytic precursor. According to NMR and DFT studies, this result is due to the peculiar behaviour of the nitrile ligand, undergoing

conversion into an anionic ligand rather than dissociation, and to the viable, reversible  $\kappa^3\text{to}\kappa^2$  coordination switching of the tpm. Alternative reaction pathways with other complexes, involving the dissociation of a neutral ligand, are less effective. Although the versatility of tpm coordination is generally accepted to play some role in related catalytic reactions, we provide here strong evidence of the importance of such feature in a hydrogenation process.

## 4. Experimental

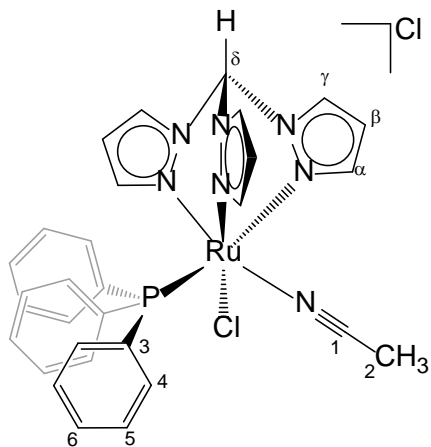
### 4.1. Materials and methods.

Reactants and solvents were purchased from Alfa Aesar, Merck, Strem or TCI Chemicals, and were of the highest purity available. Tris(1-pyrazolyl)methane (tpm) was prepared according to the published procedure.<sup>80</sup> Reactions were conducted under N<sub>2</sub> atmosphere using standard Schlenk techniques, and all products were stored in air once isolated. Solvents were used as received unless otherwise stated. Toluene and diethyl ether were dried with the solvent purification system mBraun MB SPS5, while methanol was distilled from calcium hydride and isopropanol from magnesium. IR spectra of solid samples were recorded on Agilent Cary630 FTIR spectrometer. IR spectra were processed with Spectragryph software.<sup>81</sup> NMR spectra of ruthenium complexes were recorded at 298 K on a Jeol JNM-ECZ500R instrument equipped with a Royal HFX Broadband probe, while NMR spectra of organic products were recorded at 298 K on Bruker spectrometer (300 MHz or 400 MHz). Chemical shifts (expressed in parts per million) are referenced to the residual solvent peaks (<sup>1</sup>H, <sup>13</sup>C)<sup>82</sup> or to external standard (<sup>31</sup>P to H<sub>3</sub>PO<sub>4</sub>). <sup>1</sup>H and <sup>13</sup>C{<sup>1</sup>H} NMR spectra of ruthenium complexes were assigned with the assistance of <sup>1</sup>H-<sup>13</sup>C (*gs*-HSQC and *gs*-HMBC) correlation experiments.<sup>83</sup> Elemental analyses were performed on a Vario MICRO cube instrument (Elementar).

### 4.2. Synthesis and characterization of ruthenium complexes.

**[RuCl( $\kappa^3$ -tpm)(PPh<sub>3</sub>)(NCMe)]Cl, 2 (Figure 5)**

**Figure 5.** Structure of **2**(labelling refers to carbon atoms).



A solution of **1** (200 mg, 0.22 mmol) in 25 mL of acetonitrile was heated at reflux for 3h. The solvent was evaporated under reduced pressure and the solid residue was washed with diethyl ether (25 mL) and then dried under vacuum. Yellow solid, yield 144 mg (95%). Anal. calcd. for C<sub>30</sub>H<sub>28</sub>Cl<sub>2</sub>N<sub>7</sub>PRu: C, 52.26; H, 4.09; N, 14.22; Cl, 10.28. Found: C, 52.02; H, 3.98; N, 14.26; Cl, 10.41. IR (solid state):  $\tilde{\nu}/\text{cm}^{-1}$  = 3109w, 3055w, 2958w, 2919w, 2278w ( $\tilde{\nu}_{\text{N}=\text{C}}$ ), 1620w-br, 1507w, 1483w, 1450w, 1433m, 1408m, 1375w, 1289m, 1277w, 1252w, 1223w, 1187w, 1090s, 1053w, 1048w, 997w, 987w, 857w, 971s, 779s, 767s, 750s, 756s, 695s. <sup>1</sup>H NMR (CDCl<sub>3</sub>):  $\delta/\text{ppm}$  = 12.29 (s, 1H, C<sup>δ</sup>H); 8.90, 8.75, 8.71 (d, 3H, <sup>3</sup>J<sub>HH</sub> = 2.9 Hz, C<sup>γ</sup>H); 8.14 (d-br, 1H, C<sup>α</sup>H); 6.91, 6.55 (d, 2H, <sup>3</sup>J<sub>HH</sub> = 2.2 Hz, C<sup>α</sup>H); 7.41-7.27 (m, 15H, C<sup>3</sup>H + C<sup>4</sup>H + C<sup>6</sup>H); 6.43 (s-br, 1H C<sup>β</sup>H); 6.07, 5.96 (t, 2H, <sup>3</sup>J<sub>HH</sub> = 2.6 Hz, C<sup>β</sup>H); 2.16 (s, 3H, C<sup>2</sup>H). <sup>13</sup>C{<sup>1</sup>H} NMR (CDCl<sub>3</sub>):  $\delta/\text{ppm}$  = 148.0, 147.2, 144.1 (C<sup>α</sup>); 135.6, 135.4, 133.6 (C<sup>γ</sup>); 134.1 (C<sup>4</sup>, <sup>3</sup>J<sub>PC</sub> = 9.4 Hz); 132.3 (C<sup>3</sup>, <sup>1</sup>J<sub>PC</sub> = 42.3 Hz); 130.1 (C<sup>6</sup>); 128.3 (C<sup>5</sup>, <sup>4</sup>J<sub>PC</sub> = 9.3 Hz); 127.9 (C<sup>1</sup>); 108.3, 108.2, 108.0 (C<sup>β</sup>); 74.4 (C<sup>δ</sup>); 4.7 (C<sup>2</sup>). <sup>31</sup>P{<sup>1</sup>H} NMR (CDCl<sub>3</sub>):  $\delta/\text{ppm}$  = 48.1. <sup>1</sup>H NMR (CD<sub>3</sub>OD):  $\delta/\text{ppm}$  = 8.43, 8.37, 8.35 (d, 3H, <sup>3</sup>J<sub>HH</sub> = 2.9 Hz, C<sup>γ</sup>H); 8.25, 7.03, 6.97 (d, 3H, <sup>3</sup>J<sub>HH</sub> = 2.2 Hz, C<sup>α</sup>H); 7.47 (m, 3H, C<sup>6</sup>H); 7.36 (m, 12H, C<sup>3</sup>H + C<sup>4</sup>H); 6.65, 6.32, 6.20 (t, 3H, <sup>3</sup>J<sub>HH</sub> = 2.6 Hz, C<sup>β</sup>H); 2.37 (s, 3H, C<sup>2</sup>H). C<sup>δ</sup>H not observed. <sup>13</sup>C{<sup>1</sup>H} NMR (CD<sub>3</sub>OD):  $\delta/\text{ppm}$  = 150.2, 149.6, 146.2 (C<sup>α</sup>); 136.3, 136.1, 134.2

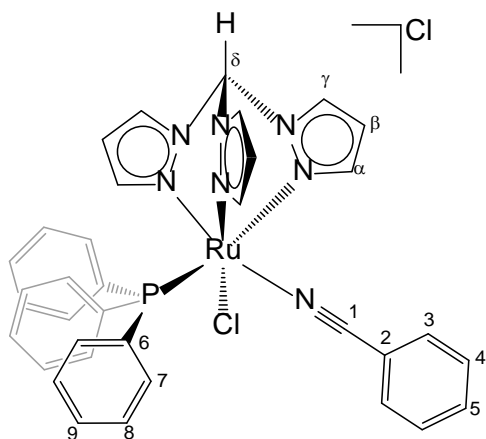
(C<sup>γ</sup>); 135.2 (C<sup>4</sup>, <sup>3</sup>J<sub>PC</sub> = 9.5 Hz); 133.3 (C<sup>3</sup>, <sup>1</sup>J<sub>PC</sub> = 42.9 Hz); 131.4 (C<sup>6</sup>); 129.4 (C<sup>5</sup>, <sup>4</sup>J<sub>PC</sub> = 9.5 Hz); 127.5 (C<sup>1</sup>); 110.0, 109.6, 109.5 (C<sup>β</sup>); 77.4 (C<sup>δ</sup>); 3.8 (C<sup>2</sup>). <sup>31</sup>P{<sup>1</sup>H} NMR (CD<sub>3</sub>OD): δ/ppm = 48.1. When a solution of **2** (0.055 mmol) and PPh<sub>3</sub> (0.055 mmol) in ethanol (4 mL) was heated at reflux for 3 hours, half conversion of **2** into **1** was finally recognized by <sup>1</sup>H and <sup>31</sup>P{<sup>1</sup>H} NMR spectra (**1/2** ratio = 1).

#### 4.3. General procedure for the synthesis of [RuCl(κ<sup>3</sup>-tpm)(PPh<sub>3</sub>)(L)]Cl.

A solution of **1** and the appropriate reagent L in ethanol was heated at reflux for a variable time. After cooling to room temperature, the volatiles were evaporated under reduced pressure. The solid residue was dissolved in the minimum volume of dichloromethane, precipitated with diethyl ether, filtered and dried under vacuum.

#### [RuCl(κ<sup>3</sup>-tpm)(PPh<sub>3</sub>)(NCPh)]Cl, **3** (Figure 6)

**Figure 6.** Structure of **3** (labelling refers to carbon atoms).



From **1** (150 mg, 0.16 mmol) and benzonitrile (20.4 μL, 0.198 mmol) in ethanol (7 mL). Reaction time: 16 h. Yellow solid, yield 116 mg (94%). Anal. calcd. for C<sub>35</sub>H<sub>30</sub>Cl<sub>2</sub>N<sub>7</sub>PRu: C, 55.93; H, 4.02; N, 13.04; Cl, 9.43. Found: C, 55.88; H, 4.16; N, 13.17; Cl, 9.36. IR (solid state):  $\tilde{\nu}/\text{cm}^{-1}$  = 3116w, 3055w, 3021w, 2907w, 2862w, 2765w, 2723w, 2678w, 2618w, 2247 ( $\tilde{\nu}_{\text{N}=\text{C}}$ ), 1653w, 1509w, 1480w, 1446m, 1436m, 1431m, 1406m, 1288m, 1248m, 1219w, 1087s, 1054m, 1047s, 999w, 987w, 888w, 856m,



6H, C<sup>5</sup>H); 6.97 (t-br, 6H, C<sup>6</sup>H); 6.90, 6.46 (m, 2H, CH<sup>Imid</sup>); 6.23 (m, 1H, C<sup>β</sup>H); 6.09, 5.99 (t, 1H, <sup>3</sup>J<sub>HH</sub> = 2.5 Hz, C<sup>β</sup>H). <sup>13</sup>C{<sup>1</sup>H} NMR (CDCl<sub>3</sub>): δ/ppm = 148.6 (C<sup>α</sup> + C<sup>α</sup> *superimposed*); 144.3 (C<sup>α</sup>); 139.8 (C<sup>Imid</sup>); 135.2, 134.3, 132.8 (C<sup>γ</sup>); 133.9 (d, <sup>3</sup>J<sub>CP</sub> = 9.3 Hz, C<sup>5</sup>); 132.8 (d, <sup>1</sup>J<sub>CP</sub> = 40.1 Hz, C<sup>4</sup>); 130.4 (C<sup>Imid</sup>); 129.8 (C<sup>7</sup>); 128.2 (d, <sup>2</sup>J<sub>CP</sub> = 9.1 Hz, C<sup>6</sup>); 116.6 (C<sup>Imid</sup>); 108.5 (C<sup>β</sup>); 108.2 (2C<sup>β</sup> *superimposed*); 74.7 (C<sup>δ</sup>). <sup>31</sup>P{<sup>1</sup>H} NMR (CDCl<sub>3</sub>): δ/ppm = 51.6. Crystals suitable for X-ray diffraction were collected by slow diffusion into diethyl ether from a dichloromethane/chloroform solution of **4**.

#### 4.4. X-ray crystallography

Crystal data and collection details for **4·solv** are reported in Table 3. Data were recorded on a Bruker APEX II diffractometer equipped with a PHOTON2 detector using Mo–K $\alpha$  radiation. The structures were solved by direct methods and refined by full-matrix least-squares based on all data using  $F^2$ .<sup>84</sup> Hydrogen atoms were fixed at calculated positions and refined using a riding model. The crystals of **4·solv** were thin plates of low quality and the data have been cut at  $2\theta = 46^\circ$ . Because of this, corrections for absorption were not very accurate and, thus, some high residual electron densities remained close to the heavy atoms, in position which are not realistic for any atom. The unit cell of **4·solv** contains an additional total potential solvent accessible void of 813 Å<sup>3</sup> (*ca.* 2% of the Cell Volume), which is likely to be occupied by highly disordered solvent and water molecules. These voids have been treated using the SQUEEZE routine of PLATON.<sup>85,86</sup>

**Table 3.** Crystal data and measurement details for **4·solv**.

	<b>4·solv</b>
Formula	C <sub>31</sub> H <sub>29</sub> Cl <sub>2</sub> N <sub>8</sub> PRu
FW	716.56
T, K	100(2)
$\lambda$ , Å	0.71073
Crystal system	Monoclinic
Space group	$P2_1/c$
$a$ , Å	11.793(4)
$b$ , Å	22.168(7)



c, Å	14.138(5)
$\beta$ , °	101.122(10)
Cell Volume, Å <sup>3</sup>	3627(2)
Z	4
$D_c$ , g·cm <sup>-3</sup>	1.312
$\mu$ , mm <sup>-1</sup>	0.655
F(000)	1456
Crystal size, mm	0.14×0.13×0.07
$\theta$ limits, °	1.732-22.998
Reflections collected	24479
Independent reflections	4929 [ $R_{int}$ = 0.1520]
Data / restraints / parameters	4929 / 522 / 388
Goodness on fit on $F^2$	1.677
$R_1$ ( $I > 2\sigma(I)$ )	0.1850
$wR_2$ (all data)	0.4462
Largest diff. peak and hole, e Å <sup>-3</sup>	8.392 / -6.570

#### 4.5. Solubility and chloride exchange in aqueous solution.

The water solubility of **2-4** was assessed by <sup>1</sup>H NMR spectroscopy (Table 4). The selected Ru compound (3-5 mg) was added to a solution of D<sub>2</sub>O (0.7 mL) containing Me<sub>2</sub>SO<sub>2</sub> as internal standard<sup>87</sup> (3.36·10<sup>-3</sup> M). The mixture was vigorously stirred at 21 °C for 2 h. The resulting saturated solution was filtered over celite, transferred into an NMR tube and analysed by <sup>1</sup>H and <sup>31</sup>P{<sup>1</sup>H} NMR spectroscopy (delay time = 3 s; number of scans = 20). The concentration (solubility) was calculated by the relative integral (starting complex + aquo-complex, C <sup>$\beta$</sup> H signal in the <sup>1</sup>H spectrum) with respect to Me<sub>2</sub>SO<sub>2</sub> ( $\delta$ /ppm = 3.14); solubility value for **3** is below the detection limit. D<sub>2</sub>O solutions of **2** and **4** were maintained at 37 °C for additional 48 hours, then <sup>1</sup>H and <sup>31</sup>P{<sup>1</sup>H} NMR analyses at RT were repeated; newly formed organometallic species were not detected. The final percentage of the aquo-complex was calculated by the relative integral of the C <sup>$\beta$</sup> H signal in the <sup>1</sup>H spectrum with respect to Me<sub>2</sub>SO<sub>2</sub> ( $\delta$ /ppm = 3.14 in D<sub>2</sub>O), see Table 4.

**Table 4.** Solubility and speciation of ruthenium complexes in D<sub>2</sub>O. <sup>a</sup>Immediately after sample preparation, t<sub>0</sub> (see above). <sup>b</sup>After maintaining the solutions at 37 °C for additional 48 h.

Compound	Solubility / 10 <sup>-3</sup> mol·L <sup>-1</sup> (D <sub>2</sub> O, 21 °C)	% aquo-species(D <sub>2</sub> O, 21 °C) <sup>a</sup>	% aquo-species(D <sub>2</sub> O, 21 °C) <sup>b</sup>
<b>2</b>	4.5	80	92
<b>3</b>	insoluble	-	-
<b>4</b>	4.0	46	94
<b>5</b>	insoluble	-	-

#### 4.6. Transfer hydrogenation reactions

In a typical procedure, a 4 mL vial equipped with a septum cap and a stirring bar was charged with ketone (0.5 mmol, 1 eq.), [RuCl( $\kappa^3$ -tpm)(PPh<sub>3</sub>)(NCMe)]Cl, **2** (3.4 mg, 1 mol%), NaOH (2.0 mg, 10 mol%), and <sup>i</sup>PrOH (2 mL). The reaction mixture was stirred at 80 °C under Ar. After 6 or 12 hours, the solvent was removed under vacuum. Purification by column chromatography on silica gel with PE/EA (v/v = 10/1~8/1) as eluting solvent to give the desired alcohol products.

$\alpha$ -Methylbenzenemethanol. <sup>1</sup>H NMR (CDCl<sub>3</sub>):  $\delta$ /ppm = 7.37 – 7.06 (m, 5H), 4.78 (q, *J* = 6.5 Hz, 1H), 2.04 (s, 1H), 1.39 (d, *J* = 6.5 Hz, 3H). <sup>13</sup>C NMR (CDCl<sub>3</sub>):  $\delta$ /ppm = 145.9, 128.6, 127.5, 125.5, 70.5, 25.2. Data agree with reported information.<sup>2c</sup>

1-(2-Methylphenyl)ethanol. <sup>1</sup>H NMR (CDCl<sub>3</sub>):  $\delta$ /ppm = 7.52 (dd, *J* = 7.5, 1.5 Hz, 1H), 7.27 – 7.22 (td, 1H), 7.18 (td, *J* = 7.3, 1.5 Hz, 1H), 7.15 – 7.12 (m, 1H), 5.13 (q, *J* = 6.4 Hz, 1H), 2.35 (s, 3H), 1.89 (s, 1H), 1.47 (d, *J* = 6.4 Hz, 3H). <sup>13</sup>C NMR (CDCl<sub>3</sub>):  $\delta$ /ppm = 144.0, 134.3, 130.5, 127.3, 126.5, 124.6, 66.9, 24.0, 19.0. Data agree with reported information.<sup>2a</sup>

1-(4-Chlorophenyl)ethanol. <sup>1</sup>H NMR (CDCl<sub>3</sub>):  $\delta$ /ppm = 7.38 – 7.09 (m, 4H), 4.82 (q, *J* = 6.5 Hz, 1H), 2.18 (s, 1H), 1.42 (d, *J* = 6.5 Hz, 3H). <sup>13</sup>C NMR (CDCl<sub>3</sub>):  $\delta$ /ppm = 144.4, 133.1, 128.7, 126.9, 69.8, 25.3. Data agree with reported information.<sup>2c</sup>

Diphenylmethanol. <sup>1</sup>H NMR (CDCl<sub>3</sub>):  $\delta$ /ppm = 7.43 – 7.11 (m, 10H), 5.75 (s, 1H), 2.23 (s, 1H). <sup>13</sup>C NMR (CDCl<sub>3</sub>):  $\delta$ /ppm = 143.9, 128.6, 127.7, 126.7, 76.4. Data agree with reported information.<sup>2c</sup>

Bis(4-methoxyphenyl)methanol.  $^1\text{H}$  NMR ( $\text{CDCl}_3$ ):  $\delta/\text{ppm}$  = 7.32 – 7.20 (m, 4H), 6.96 – 6.81 (m, 4H), 5.76 (s, 1H), 3.78 (s, 6H), 2.13 (s, 1H).  $^{13}\text{C}$  NMR ( $\text{CDCl}_3$ ):  $\delta/\text{ppm}$  = 159.1, 136.5, 127.9, 114.0, 75.5, 55.4. Data agree with reported information.<sup>2c</sup>

Bis(4-fluorophenyl)methanol.  $^1\text{H}$  NMR ( $\text{CDCl}_3$ ):  $\delta/\text{ppm}$  = 7.38 – 7.28 (m, 4H), 7.09 – 6.98 (m, 4H), 5.81 (s, 1H), 2.23 (d,  $J$  = 2.9 Hz, 1H).  $^{13}\text{C}$  NMR ( $\text{CDCl}_3$ ):  $\delta/\text{ppm}$  = 164.0, 160.8, 128.3 (d,  $J$  = 8.1 Hz), 115.6 (d,  $J$  = 21.5 Hz), 75.1. Data agree with reported information.<sup>2c</sup>

#### 4.7. NMR mechanistic studies

**Reaction of complex 2 with  $i\text{PrOH}/\text{NaOH}$ .** A mixture of complex **2** (30 mg, 0.043 mmol) and NaOH (1.9 mg, 0.048 mmol) in anhydrous isopropanol (1.5 mL) was heated at 80 °C for 1h under Ar atmosphere. After cooling to room temperature, the volatiles were evaporated under vacuum; a yellow-green solid was obtained and analysed by NMR and IR spectroscopy (Figure S5 and Figures S31a-S33a). IR (solid state, **2a**):  $\tilde{\nu}/\text{cm}^{-1}$  = 3317m-br ( $\tilde{\nu}_{\text{OH}}$ ), 3113m, 3055m, 2964m, 2918m, 2870m, 1665-1545m ( $\tilde{\nu}_{\text{C=O}}$ ), 1434m, 1406m, 1256m, 1087s, 1049m, 1023m, 856w, 787s, 748s, 692s, 607w, 526s, 506s.  $^1\text{H}$  NMR ( $\text{CD}_3\text{OD}$ , **2b**):  $\delta/\text{ppm}$  = 8.60, 8.54, 8.46 (d, 3H,  $^3J_{\text{HH}}$  = 2.9 Hz,  $\text{C}^\gamma\text{H}$ ); 8.16, 6.95, 6.95 (d, 3H,  $^3J_{\text{HH}}$  = 2.2 Hz,  $\text{C}^\alpha\text{H}$ ); 7.45 (t, 3H,  $PPh_3$ ); 7.33 (t, 6H,  $PPh_3$ ); 7.11 (t, 6H,  $PPh_3$ ); 6.69, 6.41, 6.18 (t, 3H,  $^3J_{\text{HH}}$  = 2.6 Hz,  $\text{C}^\beta\text{H}$ ); 5.68 (s-br, 1H, Ru-NHCOMe); 3.93 (sept, 1H,  $^3J_{\text{HH}}$  = 6.2 Hz, OHCHMe<sub>2</sub>); 1.94-1.93 (s, 3H, Ru-NHCOMe); 1.15 (d, 6H,  $^3J_{\text{HH}}$  = 6.2 Hz, OHCHMe<sub>2</sub>); -13.9 (d, *traces*,  $^2J_{\text{PH}}$  = 28.8 Hz, Ru-H).  $\text{C}^\delta\text{H}$  not observed.  $^{13}\text{C}\{^1\text{H}\}$  NMR ( $\text{CD}_3\text{OD}$ , **2b**):  $\delta/\text{ppm}$  = 184.4-184.3 (d, Ru-NHCOMe); 150.4, 149.1, 147.0 ( $\text{C}^\alpha$ ); 136.3, 136.2, 134.6 ( $\text{C}^\gamma$ ); 134.9 (d,  $PPh_3$ ,  $^3J_{\text{PC}}$  = 9.6 Hz); 133.7 (d,  $PPh_3$ ,  $^1J_{\text{PC}}$  = 41.2 Hz); 131.1 (d,  $PPh_3$ ,  $^4J_{\text{PC}}$  = 2.1 Hz); 129.4 (d,  $PPh_3$ ,  $^2J_{\text{PC}}$  = 9.1 Hz); 109.9, 109.8, 109.7 ( $\text{C}^\beta$ ); 64.7 (OHCHMe<sub>2</sub>); 26.1-26.0 (Ru-NHCOMe); 25.3 (OHCHMe<sub>2</sub>).  $\text{C}^\delta$  not observed.  $^{31}\text{P}\{^1\text{H}\}$  NMR ( $\text{CD}_3\text{OD}$ , **2b**):  $\delta/\text{ppm}$  = 53.3; 33.0 (*OPPh<sub>3</sub> as impurity*).  $^1\text{H}$  NMR ( $\text{CD}_2\text{Cl}_2$ ):  $\delta/\text{ppm}$  = 12.31 (s, 1H,  $\text{C}^\delta\text{H}$ ); 8.82, 8.82, 8.81 (m, 3H,  $\text{C}^\gamma\text{H}$ ); 7.93, 6.92, 6.50 (d, 3H,  $\text{C}^\alpha\text{H}$ ); 7.39 (t, 3H,  $PPh_3$ ); 7.28 (t, 6H,  $PPh_3$ ); 7.10 (t, 6H,  $PPh_3$ ); 6.41, 6.08, 6.06 (t, 3H,  $\text{C}^\beta\text{H}$ ); 4.44 (s-br, 1H, NHCOMe); 3.95 (sept, 1H,  $^3J_{\text{HH}}$  = 6.1

Hz, OHCHMe<sub>2</sub>); 1.85 (s, 3H, NHCOMe); 1.10 (d, 6H, <sup>3</sup>J<sub>HH</sub> = 6.1 Hz, OHCHMe<sub>2</sub>). <sup>31</sup>P{<sup>1</sup>H} NMR (CD<sub>2</sub>Cl<sub>2</sub>): δ/ppm = 55.82; 54.74 (**2**, 22%); 28.3 (OPPh<sub>3</sub> as impurity). Afterwards, the solvent was eliminated from the sample in CD<sub>3</sub>OD, the residue was washed with diethyl ether (3 x 4 mL) and then redissolved in CD<sub>3</sub>OD, and new NMR spectra were recorded (Figures S31b-S33b).

Then, the reaction was repeated under the conditions described above except for the addition of acetophenone (10.2 μL, 0.087 mmol), and NMR spectra were subsequently recorded (Figures S31c-S33c). <sup>1</sup>H NMR (CD<sub>3</sub>OD): δ/ppm = 8.60, 8.53, 8.45 (d, 3H, <sup>3</sup>J<sub>HH</sub> = 2.9 Hz, C<sup>γ</sup>H); 8.16, 6.95, 6.95 (d, 3H, C<sup>α</sup>H); 7.99 (d, *l*-phenylethanol); 7.61 (t, *l*-phenylethanol); 7.50 (t, *l*-phenylethanol); 7.45 (t, 3H, PPh<sub>3</sub>); 7.36-7.21 (arom, acetophenone); 7.33 (t, 6H, PPh<sub>3</sub>); 7.11 (t, 6H, PPh<sub>3</sub>); 6.69, 6.41, 6.18 (t, 3H, <sup>3</sup>J<sub>HH</sub> = 2.6 Hz, C<sup>β</sup>H); 5.68 (s-br, 1H, Ru-NHCOMe); 4.81 (q, <sup>3</sup>J<sub>HH</sub> = 6.5 Hz, *l*-phenylethanol); 3.93 (sept, 1H, <sup>3</sup>J<sub>HH</sub> = 6.2 Hz, OHCHMe<sub>2</sub>); 2.60 (s, Me, acetophenone); 1.94-1.93 (s, 1H, Ru-NHCOMe); 1.42 (d, <sup>3</sup>J<sub>HH</sub> = 6.4 Hz, Me, *l*-phenylethanol); 1.15 (d, 6H, <sup>3</sup>J<sub>HH</sub> = 6.2 Hz, OHCHMe<sub>2</sub>); -13.9 (d, traces, <sup>2</sup>J<sub>PH</sub> = 28.7 Hz, Ru-H). C<sup>δ</sup>H not observed. <sup>13</sup>C{<sup>1</sup>H} NMR (CD<sub>3</sub>OD): δ/ppm = 184.4 - 184.3 (d, Ru-NHCOMe); 150.4, 149.1, 147.0 (C<sup>α</sup>); 147.6 (arom, *l*-phenylethanol); 138.4 (arom, acetophenone); 136.3, 136.2, 134.5 (C<sup>γ</sup>); 134.9 (d, PPh<sub>3</sub>, <sup>3</sup>J<sub>PC</sub> = 9.6 Hz); 134.4 (arom, acetophenone); 133.7 (d, PPh<sub>3</sub>, <sup>1</sup>J<sub>PC</sub> = 40.9 Hz); 131.1 (d-br, PPh<sub>3</sub>); 129.7 (arom, *l*-phenylethanol); 129.4, 129.3 (arom, acetophenone); 129.4 (d, PPh<sub>3</sub>, <sup>2</sup>J<sub>PC</sub> = 9.1 Hz); 128.1 (arom, *l*-phenylethanol); 126.5 (arom, *l*-phenylethanol); 109.9, 109.8, 109.7 (C<sup>β</sup>); 70.8 (CH, *l*-phenylethanol); 64.7 (OHCHMe<sub>2</sub>); 26.7 (Me, acetophenone); 26.1-26.0 (Ru-NHCOMe); 25.6 (Me, *l*-phenylethanol); 25.3 (OHCHMe<sub>2</sub>). C<sup>δ</sup> not observed. <sup>31</sup>P{<sup>1</sup>H} NMR (CD<sub>3</sub>OD): δ/ppm = 53.3. <sup>31</sup>P{<sup>1</sup>H} NMR (CD<sub>3</sub>OD): δ/ppm = 53.3; 48.1 (**2**, 13%); 33.0 (OPPh<sub>3</sub> as impurity).

For comparison, the NMR spectra of commercial acetamide were also recorded. <sup>1</sup>H NMR (CD<sub>3</sub>OD): δ/ppm = 1.94 (s, 3H, NH<sub>2</sub>COMe). <sup>13</sup>C{<sup>1</sup>H} NMR (CD<sub>3</sub>OD): δ/ppm = 176.4 (s, NH<sub>2</sub>COMe); 22.1 (s, NH<sub>2</sub>COMe).

**Reactions of complexes 1, 3 and 4 with <sup>i</sup>PrOH/NaOH.** A mixture of the selected complex and NaOH, in anhydrous 2-propanol (1.2 mL), was heated at 80 °C for 1h under Ar atmosphere. After cooling to room temperature, the volatiles were evaporated under reduced pressure; a yellow solid was obtained and analysed by NMR spectroscopy (only relevant signals are reported in the following).

From **1** (26 mg, 0.029 mmol) and NaOH (1.3 mg, 0.032 mmol). <sup>31</sup>P{<sup>1</sup>H} NMR (CD<sub>3</sub>OD): δ/ppm = 66.9 (d, 8%); 66.1 (2%); 44.3 (31%); 39.6 (**1**, 21%); 38.5 (5%); 33.0 (OPPh<sub>3</sub>, 5%); -5.2 (PPh<sub>3</sub>, 12%).

From **3** (25 mg, 0.032 mmol) and NaOH (1.4 mg, 0.036 mmol). <sup>1</sup>H NMR (CD<sub>3</sub>OD): δ/ppm = 8.65, 8.56, 8.52 (d, 3H, C<sup>γ</sup>H); 8.17, 7.07, 6.98 (d, 3H, C<sup>α</sup>H); 7.57-7.10 (m, PPh<sub>3</sub>, Ru-NHCOPh); 6.66, 6.43, 6.24 (t, 3H, C<sup>β</sup>H); 5.92 (s-br, 1H, Ru-NHCOPh); 3.93 (sept, 1H, <sup>3</sup>J<sub>HH</sub> = 6.2 Hz, OHCHMe<sub>2</sub>); 1.15 (d, 6H, <sup>3</sup>J<sub>HH</sub> = 6.2 Hz, OHCHMe<sub>2</sub>); -13.4 (d, traces, <sup>2</sup>J<sub>PH</sub> = 28.9 Hz, Ru-H). C<sup>δ</sup>H not observed. <sup>13</sup>C{<sup>1</sup>H} NMR (CD<sub>3</sub>OD): δ/ppm = 182.3 (Ru-NHCOPh); 64.7 (OHCHMe<sub>2</sub>); 25.3 (OHCHMe<sub>2</sub>). <sup>31</sup>P{<sup>1</sup>H} NMR (CD<sub>3</sub>OD): δ/ppm = 53.0 (73%); 47.4 (**3**, 27%).

From **4** (30 mg, 0.042 mmol) and NaOH (1.8 mg, 0.046 mmol). <sup>31</sup>P{<sup>1</sup>H} NMR (CD<sub>3</sub>OD): δ/ppm = 54.9 (22%); 52.9 (61%); 51.7 (8%); 51.5 (9%).

#### 4.8. Computational details

All geometries were optimized with ORCA 5.0.3, using the B97 functional with the zero-order regular approximation (ZORA) to take relativistic effects into account and in conjunction with a triple-ζ quality basis set (ZORA-TZVP). For ruthenium, the basis set “old-ZORA-TZVP” has been used. The dispersion corrections were introduced using the Grimme D3-parametrized correction and the Becke Johnson damping to the DFT energy. All the structures were confirmed to be local energy minima (no imaginary frequencies), or saddle points (one imaginary frequency corresponding to the reaction coordinate). The solvent was considered through the continuum-like polarizable continuum model (C-PCM, isopropanol).

## **Acknowledgements**

We thank the University of Pisa for financial support (Fondi di Ateneo 2021). We gratefully acknowledge VLAIO (SBO project CO2PERATE) and the Special Research Fund (BOF) of Ghent University. X. M. thanks the CSC (China Scholarship Council) for PhD fellowships.

## **Supporting Information Available**

IR and NMR spectra of ruthenium complexes; catalytic studies; NMR spectra for mechanistic studies; DFT calculations. CCDC reference number 2168078 (**4**) contains the supplementary crystallographic data for the X-ray study reported in this work. This data is available free of charge at <http://www.ccdc.cam.ac.uk/structures>.

## **Author contributions**

The project was designed by FM and SN. AG performed the synthesis and the characterization of the complexes, and NMR studies. LB and MG assisted the synthetic work. GC performed the DFT calculations. SZ solved the single-crystal X-ray crystallography structure. XM executed the catalysis experiments. GP, SN and FM provided funding. AG, XM, GC, SN and FM wrote the manuscript.

**The authors declare no competing financial interests.**

**Keywords:** Ruthenium(II) complexes; tris(pyrazol-1-yl)methane; catalysis; transfer hydrogenation; coordination switching.

## **References**

- 
- 1 X. Zhang, P.-L. Shao, Edited by V. Ratovelomanana-Vidal, P. Phansavath, *From Asymmetric Hydrogenation and Transfer Hydrogenation* 2021, 175-219.
  - 2 C. Pettinari, F. Marchetti, D. Martini, Edited by J. A. McCleverty, T. J. Meyer, *Comprehensive Coordination Chemistry II* 2004, 9, 75-139.
  - 3 D. Wang, D. Astruc, *The Golden Age of Transfer Hydrogenation*. *Chem. Rev.* 2015, 115, 6621-6686.
  - 4 D. Baidilov, D. Hayrapetyan, A. Y. Khalimon, Recent advances in homogeneous base-metal-catalyzed transfer hydrogenation reactions. *Tetrahedron* 2021, 98, 132435.
  - 5 M. K. Whittlesey, *Transfer hydrogenation*. Edited by S. P. Nolan, C. S. Cazin, *Science of Synthesis, N-Heterocyclic Carbenes in Catalytic Organic Synthesis*, 2017, 1, 285-300.
  - 6 V. B. Kharitonov, D. V. Muratov, D. A. Loginov, Cyclopentadienyl complexes of group 9 metals in the total synthesis of natural products, *Coord. Chem. Rev.* 2022, 471, 214744.
  - 7 G. Bresciani, E. Antico, G. Ciancaleoni, S. Zacchini, G. Pampaloni, F. Marchetti, Bypassing the Inertness of Aziridine/CO<sub>2</sub> Systems to Access 5-Aryl-2-Oxazolidinones: Catalyst-Free Synthesis Under Ambient Conditions, *ChemSusChem* 2020, 13, 5586-5594.
  - 8 W. Panjapakkul, M. M. El-Halwagi, Technoeconomic Analysis of Alternative Pathways of Isopropanol Production, *ACS Sustainable Chem. Eng.* 2018, 6, 10260–10272.
  - 9 J. Yu, J. Long, Y. Yang, W. Wu, P. Xue, L. W. Chung, X.-Q. Dong, X. Zhang, Iridium-Catalyzed Asymmetric Hydrogenation of Ketones with Accessible and Modular Ferrocene-Based Amino-phosphine Acid (f-Ampha) Ligands. *Org. Lett.*, 2017, 19, 3, 690–693.
  - 10 R. Wang, X. Han, J. Xu, P. Liu, F. Li, Transfer Hydrogenation of Ketones and Imines with Methanol under Base-Free Conditions Catalyzed by an Anionic Metal–Ligand Bifunctional Iridium Catalyst. *J. Org. Chem.*, 2020, 85, 2242–2249.
  - 11 R. M. Betancourt, P. Phansavath, V. Ratovelomanana-Vidal, Rhodium-Catalyzed Asymmetric Transfer Hydrogenation/Dynamic Kinetic Resolution of 3-Benzylidene-Chromanones. *Org. Lett.*, 2021, 23, 1621–1625.
  - 12 C. S. G. Seo, R. H. Morris, *Catalytic Homogeneous Asymmetric Hydrogenation: Successes and Opportunities*, *Organometallics* 2019, 38, 47–65.
  - 13 D. Wei, C. Darcel, Iron Catalysis in Reduction and Hydrometalation Reactions, *Chem. Rev.* 2019, 119, 2550-2610.

- 
- 14 Y.-Y. Li, S.-L. Yu, W.-Y. Shen, J.-X. Gao, Iron, Cobalt and Nickel-Catalyzed Asymmetric Transfer Hydrogenation and Asymmetric Hydrogenation of Ketones, *Acc. Chem. Res.* 2015, 48, 2587–2598.
  - 15 G. Talavera, A. Santana Farina, A. Zanotti-Gerosa, H.G. Nedden, Structural Diversity in Ruthenium-Catalyzed Asymmetric Transfer Hydrogenation Reactions. *Topics in Organometallic Chemistry* 2019, 65, 73-114.
  - 16 A. E. Cotman, Escaping from Flatland: Stereoconvergent Synthesis of Three-Dimensional Scaffolds via Ruthenium(II)-Catalyzed Noyori-Ikariya Transfer Hydrogenation. *Chem. Eur. J.* 2021, 27, 39-53.
  - 17 Hey, D. A.; Reich, R. M.; Baratta, W.; Kuehn, F. E. Current advances on ruthenium(II) N-heterocyclic carbenes in hydrogenation reactions. *Coord. Chem. Rev.* 2018, 374, 114-132.
  - 18 Sato, H.; Turnbull, B. W. H.; Fukaya, K.; Krische, M. J. Ruthenium(0)-Catalyzed Cycloaddition of 1,2-Diols, Ketols, or Diones via Alcohol-Mediated Hydrogen Transfer. *Angew. Chem. Int. Ed.* 2018, 57, 3012-3021.
  - 19 W. S. Knowles, R. Noyori, Pioneering Perspectives on Asymmetric Hydrogenation, *Acc. Chem. Res.* 2007, 40, 1238-1239.
  - 20 Mannu, A.; Grabulosa, A.; Baldino, S. Transfer hydrogenation from 2-propanol to acetophenone catalyzed by  $[\text{RuCl}_2(\eta^6\text{-arene})\text{P}]$  (P = monophosphine) and  $[\text{Rh}(\text{PP})_2]\text{X}$  (PP = diphosphine, X =  $\text{Cl}^-$ ,  $\text{BF}_4^-$ ) complexes. *Catalysts* 2020, 10, 162.
  - 21 Matuska, O.; Kindl, M.; Kacer, P. Edited by Ravanchi, M. T. *From New Advances in Hydrogenation Processes: Fundamentals and Applications*, 2017, 37-55.
  - 22 Suss-Fink, G. Water-soluble arene ruthenium complexes: From serendipity to catalysis and drug design. *J. Organomet. Chem.* 2014, 751, 2-19.
  - 23 P. Kumar, R. K. Gupta, D. Shankar Pandey, Half-sandwich arene ruthenium complexes: synthetic strategies and relevance in catalysis, *Chem. Soc. Rev.*, 2014, 43, 707-733.
  - 24 Hall, A. M. R.; Berry, D. B. G.; Crossley, J. N.; Codina, A.; Clegg, I.; Lowe, J. P.; Buchard, A.; Hintermair, U. *ACS Catal.* 2021, 11, 13649-13659.
  - 25 Gichumbi, J. M.; Friedrich, H. B.; Omondi, B. J. Application of arene ruthenium(II) complexes with pyridine-2-carboxaldehyde ligands in the transfer hydrogenation of ketones. *Mol. Catal. A* 2016, 416, 29-38.
  - 26 Matsuoka, A.; Sandoval, C. A.; Uchiyama, M.; Noyori, R.; Naka, H. *Chem. Asian J.* 2015, 10, 112-115.
  - 27 Steward, K. M.; Gentry, E. C.; Johnson, J. S. Dynamic Kinetic Resolution of  $\alpha$ -Keto Esters via Asymmetric Transfer Hydrogenation. *J. Am. Chem. Soc.* 2012, 134, 7329-7332.
  - 28 Ma, X.; Guillet, S. G.; Liu, Y.; Cazin, C. S. J.; Nolan, S. P. Simple synthesis of  $[\text{Ru}(\text{CO})_3(\text{NHC})(\text{p-cymene})]$  complexes and their use in transfer hydrogenation catalysis. *Dalton Trans.*, 2021, 50, 13012–13019.



- 
- 29 T. Touge, H. Nara, M. Fujiwhara, Y. Kayaki, T. Ikariya, Efficient Access to Chiral Benzhydrols via Asymmetric TransferHydrogenation of Unsymmetrical Benzophenones with BifunctionalOxo-Tethered Ruthenium Catalysts. *J. Am. Chem. Soc.*, 2016, 138, 10084–10087.
- 30 V. V. Matveevskaya, D. I. Pavlov, T. S. Sukhikh, A. L. Gushchin, A. Y. Ivanov, T. B. Tennikova, V. V. Sharoyko, S. V. Baykov, E. Benassi, A. S. Potapov, Arene–Ruthenium(II) Complexes Containing 11H-Indeno[1,2-b]quinoxalin-11-one Derivatives and Tryptanthrin6-oxime: Synthesis, Characterization, Cytotoxicity, and CatalyticTransfer Hydrogenation of Aryl Ketones. *ACS Omega*, 2020, 5, 11167–11179.
- 31 V. V. Matveevskaya, D. I. Pavlov, D. G. Samsonenko, E. A. Ermakova, L. S. Klyushova, S. V. Baykov, V. P. Boyarskiy, A. S. Potapov, Synthesis and Structural Characterization of Half-Sandwich Arene–Ruthenium(II) Complexes withBis(imidazol-1-yl)methane, Imidazole and Benzimidazole. *Inorganics*, 2021, 9, 34.
- 32 Bigmore, H. R.; Lawrence, S. C.; Mountford, P.; Tredget, C. S. Coordination, organometallic and related chemistry of tris(pyrazolyl)methane ligands. *Dalton Trans.* 2005, 635–651..
- 33 Reger, D. L. Tris(pyrazolyl)methane ligands: the neutral analogs of tris(pyrazolyl)borate ligands. *Comments on Inorganic Chemistry* 1999, 21, 1-28.
- 34 R. F. Semeniuc, D. L. Reger, Metal Complexes of Multitopic, Third Generation Poly(pyrazolyl)-methane Ligands: Multiple Coordination Arrangements, *Eur. J. Inorg. Chem.* 2016, 2253–2271.
- 35 Bhambri, S.; Tocher, D.A. Synthesis and characterisation of ruthenium(II) arene complexes containing  $\kappa^3$ - and  $\kappa^2$ -poly(pyrazolyl)borates and methanes. *J. Chem. Soc. Dalton Trans.* 1997, 18, 3367–3372.
- 36 I. Honzíčková, J. Honzíček, J. Vinklárěk and Z. Padělková, Allyl molybdenum(II) and tungsten(II) compounds bearing bidentate and tridentate pyrazolylmethane ligands, *Polyhedron*, 2014, 81, 364-369.
- 37 Munoz-Molina, J. M.; Belderrain, T. R.; Perez, P. J. Group 11 tris(pyrazolyl)methane complexes: structural features and catalytic applications. *Dalton Trans.* 2019, 48, 10772-10781.
- 38 Martins, L. M.D.R.S.; Pombeiro, A. J. L.; Tris(pyrazol-1-yl)methane metal complexes for catalytic mild oxidative functionalizations of alkanes, alkenes and ketones. *Coord. Chem. Rev.* 2014, 265, 74–88.
- 39 A. P. C. Ribeiro, L. M. D. R. S. Martins, M. L. Kuznetsov, A. J. L. Pombeiro, Tuning Cyclohexane Oxidation: Combination of Microwave Irradiation and Ionic Liquid with the C-Scorpionate [FeCl<sub>2</sub>(Tpm)] Catalyst *Organometallics* 2017, 36, 192–198.
- 40 Martins, L.M.D.R.S. C-scorpionate complexes: Ever young catalytic tools. *Coord. Chem. Rev.* 2019, 396, 89–102.
- 41 C. M. Nagaraja, MunirathinamNethaji, and Balaji R. Jagirdar, Tris(pyrazolyl)methane Sulfonate Complexes of Iridium: Catalytic Hydrogenation of 3,3-Dimethyl-1-butene, *Organometallics* 2007, 26, 6307-6311.

- 42 Poater, A.; Falivene, L.; Cavallo, L.; Llobet, A.; Rodriguez, M.; Romero, I.; Sola, M. Electronic structure and catalytic aspects of  $[\text{Ru}(\text{tpm})(\text{bqdi})(\text{Cl}/\text{H}_2\text{O})]_n$ , tpm = tris(1-pyrazolyl)methane and bqdi = o-benzoquinonediimine. *Chem. Phys. Lett.* 2013, 577, 142-146.
- 43 Serrano, I.; Lopez, M. I.; Ferrer, I.; Poater, A.; Parella, T.; Fontrodona, X.; Sola, M.; Llobet, A.; Rodriguez, M.; Romero, I. New Ru(II) Complexes Containing Oxazoline Ligands As Epoxidation Catalysts. Influence of the Substituents on the Catalytic Performance. *Inorg. Chem.* 2011, 50, 6044-6054.
- 44 Agarwala, H.; Ehret, F.; Chowdhury, A. D.; Maji, S.; Mobin, S. M.; Kaim, W.; Lahiri, G. K. Electronic structure and catalytic aspects of  $[\text{Ru}(\text{tpm})(\text{bqdi})(\text{Cl}/\text{H}_2\text{O})]_n$ , tpm = tris(1-pyrazolyl)methane and bqdi = o-benzoquinonediimine. *Dalton Trans.* 2013, 42, 3721-3734.
- 45 Yamaguchi, M.; Tomizawa, M.; Takagaki, K.; Shimo, M.; Masui, D.; Yamagishi, T. Photooxidation of alkane under visible light irradiation catalyzed by ruthenium complexes. *Catalysis Today* 2006, 117, 206-209.
- 46 M. Yamaguchi, T. Iida and T. Yamagishi, Syntheses of mixed-ligand ruthenium(II) complexes with a terpyridine or a tris (pyrazolyl)methane and a bidentate ligand: their application for catalytic hydroxylation of alkanes, *Inorg. Chem. Commun.*, 1998, 1, 299-301.
- 47 G. R. Morello, T. R. Cundari, T. Brent Gunnoe, DFT study of group 8 catalysts for the hydrophenylation of ethylene: Influence of ancillary ligands and metal identity, *J. Organomet. Chem.* 2012, 697, 15-22.
- 48 H.-J. Xu, Y. Cheng, J.-F. Sun, B. A. Dougan, Y.-Z. Li, X.-T. Chen, Z.-L. Xue, Preparation, characterization, and catalytic properties of ruthenium nitrosyl complexes with polypyrazolylmethane ligands. *J. Organomet. Chem.* 2008, 693, 3851-3857.
- 49 The synthesis of  $[\text{RuCl}_3(\text{NO})]$  was previously described but no yield was reported: Fortney, C. F.; Shepherd, R. E. Synthesis and characterization of a new  $\{\text{RuNO}\}$  complex,  $[\text{Ru}(\text{NO})(\text{bpb})\text{Cl}]$  (bpb = N,N'-bis(2-pyridinecarboxamide)-1,2-benzene dianion). *Inorg. Chem. Commun.* 2004, 7, 1065-1070.
- 50 Cervinka, J.; Gobbo, A.; Biancalana, L.; Markova, L.; Novohradsky, V.; Guelfi, M.; Zacchini, S.; Kasparkova, J.; Brabec, V.; Marchetti, F. Ruthenium(II) Tris-Pyrazolylmethane Complexes Inhibit Cancer Cell Growth by Disrupting Mitochondrial Calcium Homeostasis, *J. Med. Chem.* 2022, 65, 10567-10587.
- 51 L. D. Field, B. A. Messerle, L. Soler, I. E. Buys, T. W. Hambley, Polypyrazolylmethane complexes of ruthenium, *J. Chem. Soc., Dalton Trans.*, 2001, 1959-1965.
- 52 R. G. Belli, Y. Wu, H. Ji, A. Joshi, L. P. E. Yunker, J. S. McIndoe, L. Rosenberg, Competitive Ligand Exchange and Dissociation in Ru Indenyl Complexes. *Inorg. Chem.* 2019, 58, 747-755.
- 53 Lentz, D.; Michael-Schulz, H., Syntheses, structure determination and reactions of phosphine substituted derivatives of  $(\mu_3\text{-FC})_2\text{Fe}_3(\text{CO})_9$ . *Z. Anorg. Allg. Chem.* 1992, 618, 111-120.

- 
- 54 G. Bresciani, L. Biancalana, G. Pampaloni, S. Zacchini, G. Ciancaleoni, F. Marchetti, A Comprehensive Analysis of the Metal–Nitrile Bonding in an Organo-Diiron System, *Molecules* 2021, 26, 7088.
- 55 P. K. Baker, M. E. Harman, M. B. Hursthouse, A. I. Karaulov, A. J. Lavery, K. M. A. Malik, D. J. Muldoon, A. Shawcross, Nitrile exchange reactions of  $ML_2(CO)_3(NCMe)_2$ . X-ray crystal structures of mixed-ligand seven-coordinate complexes. *J. Organomet. Chem.* 1995, 494, 205-221.
- 56 Su, B.-K.; Liu, Y.-H.; Peng, S.-M.; Liu, S.-T. An Anthryridine-Based Pentanitrogen Donor Switches from Mono- to Tetradentate with Pd(II) Ions. *Organometallics* 2021, 40, 4110-4119.
- 57 A. P. Shaw, B. L. Ryland, J. R. Norton, D. Buccella, A. Moscatelli, Electron Exchange Involving a Sulfur-Stabilized Ruthenium Radical Cation. *Inorg. Chem.*, 2007, 46, 5805–5812.
- 58 P. S. Hallman, T. A. Stephenson, G. Wilkinson, Tetrakis (triphenylphosphine) dichlororuthenium (II) and Tris (triphenylphosphine) dichlororuthenium (II) *Inorg. Synth.*, 1970, 12, 237-240.
- 59 D. C. Wilson, J. H. Nelson, Reactions of ruthenium(II) tris(pyrazolyl)borate and tris(pyrazolyl)methane complexes with diphenylvinylphosphine and 3,4-dimethyl-1-phenylphosphole, *J. Organomet. Chem.* 2003, 682, 272-289.
- <sup>60</sup> R. S. Ramón, S. Gaillard, A. Poater, L. Cavallo,; A. M. Z. Slawin, S. P. Nolan,  $[Au(IPr)]_2(\mu-OH)X$  Complexes: Synthetic, Structural and Catalytic Studies. *Chem. Eur. J.*, 2011, 17, 1238-1246.
- 61 M. F. Ibarra-Vazquez, J. G. Alvarado-Rodríguez, A. C. Esqueda, I. I. Rangel-Salas, O. Serrano, Synthesis, structural characterization, and activity on the transfer hydrogenation reaction of dimesitylacetate piano stool organometallic complexes of Ru(II), Rh(III), and Ir(III), *J. Mol. Struct.* 2019, 1191, 52-58.
- 62 R. J. Citta, B. L. Koteles, B. Delgado-Perez, B. C. Chan, S. E. Kalman, Ruthenium(II) Complexes of an Imidazole Carboxamido Ligand for Base-Free Transfer Hydrogenation in Air, *Organometallics* 2022, 41, 3004–3013.
- 63 A. Azua, M. Finn, H. Yi, A. B. Dantas, and A. Voutchkova-Kostal, Transfer Hydrogenation from Glycerol: Activity and Recyclability of Iridium and Ruthenium Sulfonate-Functionalized N-Heterocyclic Carbene Catalysts. *ACS Sustainable Chem. Eng.* 2017, 5, 3963–3972.
- 64 K. Polborn, K. Severin, Biomimetic Catalysis with Immobilized Organometallic Ruthenium Complexes: Substrate- and Regioselective Transfer Hydrogenation of Ketones. *Chem. Eur. J.*, 2000, 6, 4604-4611.
- 65 Singh, K.; Sarbajna, A.; Dutta, I.; Pandey, P.; Bera, J. K.; Hemilability-Driven Water Activation: A Ni(II) Catalyst for Base-Free Hydration of Nitriles to Amides. *Chem. Eur. J.* 2017, 23, 7761-7771.
- 66 Ounkham, W. L.; Weeden, J. A.; Frost, B. J.; Aqueous-Phase Nitrile Hydration Catalyzed by an In Situ Generated Air-Stable Ruthenium Catalyst. *Chem. Eur. J.* 2019, 25, 10013-10020.

- 67 Guo, B.; de Vries, J. G.; Otten, E.; Hydration of nitriles using a metal–ligand cooperative ruthenium pincer catalyst. *Chem. Sci.* 2019, 10, 10647-10652.
- 68 Gonzalez-Fernandez, R.; Crochet, P.; Cadierno, V.; Arene-ruthenium(II) and osmium(II) complexes as catalysts for nitrile hydration and aldoxime rearrangement reactions. *InorgChim Acta* 2020, 517, 120180.
- 69 Knapp, S. M. M.; Sherbow, T. J.; Yelle, R. B.; Zakharov, L. N.; Juliette, J. J.; Tyler, D. R.; Mechanistic Investigations and Secondary Coordination Sphere Effects in the Hydration of Nitriles with  $[\text{Ru}(\eta^6\text{-arene})\text{Cl}_2\text{PR}_3]$  Complexes. *Organometallics* 2013, 32, 824-834.
- 70 C. S. Yi, Z. He, Transfer Hydrogenation of Carbonyl Compounds Catalyzed by a Ruthenium - Acetamido Complex: Evidence for a Stepwise Hydrogen Transfer Mechanism. *Organometallics*, 2001, 20, 3641-3643.
- 71 C. W. Leung, W. Zheng, D. Wang, S. M. Ng, C. H. Yeung, Z. Zhou, Z. Lin, C. P. Lau, Catalytic H/D Exchange between Organic Compounds and  $\text{D}_2\text{O}$  with  $\text{TpRu}(\text{PPh}_3)(\text{CH}_3\text{CN})\text{H}(\text{Tp})\text{hydro}(\text{trispyrazolyl})\text{borate}$ . Reaction of  $\text{TpRu}(\text{PPh}_3)(\text{CH}_3\text{CN})\text{H}$  with Water to Form Acetamido Complex  $\text{TpRu}(\text{PPh}_3)(\text{H}_2\text{O})(\text{NHC}(\text{O})\text{CH}_3)$ . *Organometallics*, 2007, 26, 1924-1933.
- 72 Cheung, W-. M.; Yeung, K. C. A.; Wong, K-. H.; So, Y-. M.; Sung, H. H. Y.; Williams, I. D.; Leung, W-. H.; Reactions of cerium complexes with transition metal nitrides: synthesis and structure of heterometallic cerium complexes containing bridging catecholate ligands. *Dalton Trans.* 2019, 48, 13458 -13465.
- 73 Fuma, Y.; Ebihara, M.; Tetra- $\mu$ -acetamidato- $\kappa^4\text{N}:\text{O};\kappa^4\text{O}:\text{N}$ -bis-[aqua-ruthenium(II,III)]( $\text{Ru}-\text{Ru}$ ) tetra-phenyl-borate monohydrate. *Acta Cryst.* 2006, E62, m2808-m2810.
- 74 H. S. Chu, Z. Xu, S. M. Ng, C. P. Lau, Z. Lin, Protonation of  $[\text{tpmRu}(\text{PPh}_3)_2\text{H}]\text{BF}_4$  [ $\text{tpm}$  =  $\text{Tris}(\text{pyrazolyl})\text{methane}$ ] – Formation of Unusual Hydrogen-Bonded Species. *Eur. J. Inorg. Chem.* 2000, 993.
- 75 (a) Y.-H. Chang, W.-J. Leu, A. Datta, H.-C. Hsiao, C.-H. Lin, J.-H. Guh, J.-H. Huang, Catalytic transfer hydrogenation and anticancer activity of arene – ruthenium compounds incorporating bi-dentate precursors, *Dalton Trans.*, 2015, 44, 16107–16118. (b) M. Bortoluzzi, G. Bresciani, F. Marchetti, G. Pampaloni, S. Zacchini,  $\text{MoCl}_5$  as an effective chlorinating agent towards  $\alpha$ -amino acids: synthesis of  $\alpha$ -ammonium-acylchloride salts and  $\alpha$ -amino-acylchloride complexes, *Dalton Trans.* 2015, 44, 10030–10037.
- 76 Serrano, I.; Sala, X.; Plantalech, E.; Rodriguez, M.; Romero, I.; Jansat, S.; Gomez, M.; Parella, T.; Stoeckli-Evans, H.; Solans, X.; Font-Bardia, M.; Vidjayacoumar, B.; Llobet, A.; Synthesis, Structure, Redox Properties, and Catalytic Activity of New Ruthenium Complexes Containing Neutral or Anionic and Facial or Meridional Ligands: An Evaluation of Electronic and Geometrical Effects. *Inorg. Chem.* 2007, 46, 5381-5389.
- 77 Few piano-stool ruthenium(II) complexes with monodentate anionic oxygen ligands have been isolated:(a) X.Tan,X. Hou, T. Rogge, L. Ackermann, Ruthenaelectro-Catalyzed Domino Three-Component Alkyne Annulation for Expedient Isoquinoline Assembly, *Angew. Chem. Int. Ed.* 2021, 60, 4619-4624. (b) E. V.

- 
- Mutseneck, C. Reus, F.Schödel, M. Bolte, H.-W. Lerner, M. Wagner, Reactions of  $[\text{Cp}^*\text{RuCl}]_4$  and  $[(\text{p-cymene})\text{RuCl}_2]_2$  with the Tridentate Ligand  $[\text{Ph}(\text{pz})\text{B}(\mu\text{-O})(\mu\text{-pz})\text{B}(\text{pz})\text{Ph}]^-$ , *Organometallics* 2010, 29, 966–975. (c) G. Bresciani, N. Busto, V. Ceccherini, M. Bortoluzzi, G. Pampaloni, B. Garcia, F. Marchetti, Screening the biological properties of transition metal carbamates reveals gold(I) and silver(I) complexes as potent cytotoxic and antimicrobial agents, *J. Inorg.Biochem.* 2022, 227, 111667.
- <sup>78</sup> A. de Palo, G. La Ganga, F. Nastasi, M. Guelfi, M. Bortoluzzi, G. Pampaloni, F. Puntoriero, S. Campagna, F. Marchetti, Ru(II) water oxidation catalysts with 2,3-bis(2-pyridyl)pyrazine and tris(pyrazolyl)methane ligands: assembly of photo-active and catalytically active subunits in a dinuclear structure. *Dalton Trans.*, 2020, 49, 3341-3352.
- 79 F. Fagalde, N. L. de Katz, N. Katz, Benzonitrile Hydrolysis Catalyzed by a Ruthenium(II) Complex. *J. Coord. Chem.*, 2002, 55, 587-593.
- 80 D. L. Reger, Syntheses of tris(pyrazolyl)methane ligands and  $\{[\text{tris}(\text{pyrazolyl})\text{methane}]\text{Mn}(\text{CO})_3\}\text{SO}_3\text{CF}_3$  complexes: comparison of ligand donor properties. *J. Organomet. Chem.*, 2000, 607, 120–128.
- 81 F. Menges, "Spectragryph - optical spectroscopy software", Version 1.2.5, @ 2016-2017, <http://www.effemm2.de/spectragryph>.
- 82 G. R. Fulmer, A. J. M. Miller, N. H. Sherden, H. E. Gottlieb, A. Nudelman, B. M. Stoltz, J. E. Bercaw, K. I. Goldberg, NMR Chemical Shifts of Trace Impurities: Common Laboratory Solvents, Organics, and Gases in Deuterated Solvents Relevant to the Organometallic Chemist. *Organometallics*, 2010, 29, 2176–2179.
- 83 W. Willker, D. Leibfritz, R. Kerssebaum, W. Bermel, Gradient selection in inverse heteronuclear correlation spectroscopy. *Magn. Reson. Chem.*, 1993, 31, 287-292.
- 84 G. M. Sheldrick, Crystal structure refinement with SHELXL. *Acta Crystallogr. C* 2015, 71, 3-8.
- 85 A. L. Spek, Single-crystal structure validation with the program PLATON. *J. Appl. Cryst.*, 2003, 36, 7-13.
- 86 A. L. Spek, Structure validation in chemical crystallography. *Acta Cryst.*, 2009, D65, 148-155.
- 87 T. Rundlöf, M. Mathiasson, S. Bekiroglu, B. Hakkarainen, T. Bowden, T. Arvidsson, *J. Pharm. Biomed. Anal.*, 2010, 52, 645–651.